



# *Radar Detection, Performance Analysis, and CFAR Techniques*

**Prof. Antonio De Maio (PhD, IEEE Fellow)**

E-mail: [ademaio@unina.it](mailto:ademaio@unina.it)

Tel. +390817683101

**Dr. Augusto Aubry (PhD, IEEE Senior)**

E-mail: [augusto.aubry@unina.it](mailto:augusto.aubry@unina.it)

Tel. +390817683810

DIETI, University of Napoli "Federico II"

DIETI, University of Napoli "Federico II"

**T- 03 – 2018 IEEE Radar Conference  
23 April 2018, Oklahoma City, OK, USA**



# OUTLINE OF THE TUTORIAL

This tutorial is mainly composed of two parts:

- 1) Part 1: Basic Theory of Radar Detection**
- 2) Part 2: CFAR Techniques**

## Part 1 Topics

- Data Collection: Fast-Time Slow-Time Radar Data Matrix
- Statistical Characterization of the Radar Observations
- Coherent, Non-Coherent, and Binary Integration
- Optimum Detection in Additive White Gaussian Noise (AWGN)
- False Alarm and Detection Probability Analysis
- The case of Fluctuating Targets According to Swerling 1- 4 Models
- Relevant Integrals for Performance Analysis
- Frequency Agility Issues
- MATLAB Simulation of Radar Detectors via Monte Carlo Techniques



# OUTLINE OF THE TUTORIAL

## Part 2 Topics

- The Constant False Alarm Rate (CFAR) Concept
- Basic CFAR Architecture
- Cell Averaging (CA-CFAR)
- CFAR Loss and Masking Effects
- Clutter Edges
- Robust CFAR Processors
- Greatest Of CFAR (GO-CFAR)
- Smallest Of CFAR (SO-CFAR)
- Trimmed-Mean (TM-CFAR) and Censored CFAR (CS-CFAR)
- OS-CFAR
- CFAR and Invariance

# PURPOSE AND PRE-REQUISITES OF THE TUTORIAL



**Purpose of the tutorial:** to give a rigorous and **academic point of view** on the fundamentals of radar detection, receiver performance analysis, Monte Carlo simulation of radar receivers, and CFAR algorithms. The idea is to provide a formative and methodological tutorial on the above topics which represent the base to address more challenging radar detection problems.

**Pre-Requisites:** Radar Systems Fundamentals, Basic Probability and Statistical Theory, Mathematical Analysis.

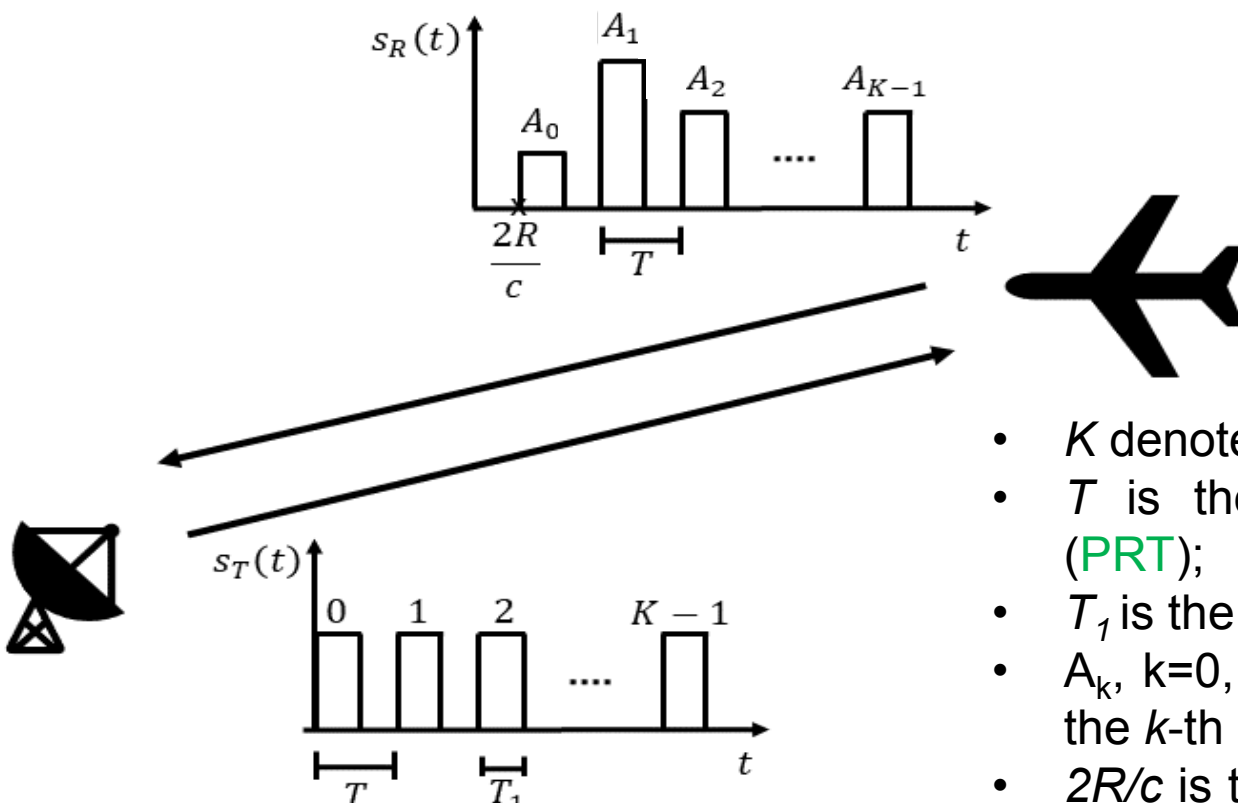


*Part 1 :*  
*Basic Theory of*  
*Radar Detection*



# PROBLEM FORMULATION

Let us consider a stationary **mono-static radar system** which transmits a possibly modulated burst of pulses and collects data from a given azimuth-elevation cell during a time interval usually referred to as dwell time.



- $K$  denotes the **number of pulses**;
- $T$  is the Pulse Repetition Time (**PRT**);
- $T_1$  is the **pulse length**;
- $A_k$ ,  $k=0,\dots,K-1$ , is the amplitude of the  $k$ -th return pulse;
- $2R/c$  is the **round trip delay**, where  $R$  is the target range.



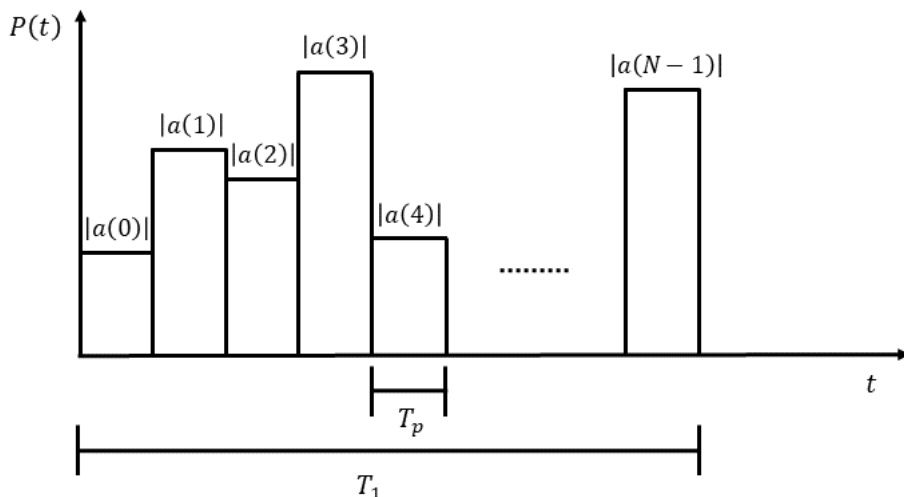
# PROBLEM FORMULATION

The Radio Frequency (RF) transmitted signal can be expressed as

$$s_T(t) = \sqrt{P_T} \sum_{k=0}^{K-1} p(t - kT) e^{j2\pi f_0 t}$$

where  $P_T$  rules the radar transmitted power,  $f_0$  is the **carrier** frequency, and  $p(t)$  represents the baseband equivalent of the generic **pulse** with length  $T_1$ , i.e.,

$$p(t) = \sum_{i=0}^{N-1} a(i) u(t - iT_p),$$



- $a(i)$ ,  $i = 0, \dots, N - 1$ , are the radar code elements;
- $u(t)$  is the **chip pulse** (or sub-pulse) baseband equivalent;
- $T_p = T_1 / N$  is the length of  $u(t)$ ;
- the energy of  $u(t)$  is assumed (without loss of generality) unitary.



# PROBLEM FORMULATION

The baseband equivalent of the received signal can be expressed as

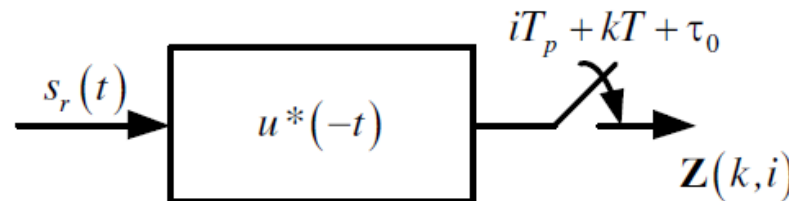
$$s_r(t) = e^{-j2\pi f_0 \tau_0} \sum_{k=0}^{K-1} A_k e^{j\phi_k} p(t - kT - \tau_0) e^{j2\pi f_d(t-\tau_0)} + n(t)$$

- $f_d$  is the target **Doppler frequency** which is related to the **radial velocity**  $v_r$  through the equation  $f_d = 2\nu_r/\lambda$  with  $\lambda$  the carrier wavelength;
- $\tau_0 = 2R/c$  is the **round trip delay**;
- the **complex amplitudes**  $A_k e^{j\phi_k}$ ,  $k = 0, \dots, K - 1$ , are unknown parameters accounting for the target Radar Cross Section (**RCS**), channel propagation effects, and other terms involved into the radar range equation. If  $A_k e^{j\phi_k} = A e^{j\phi}$ ,  $k = 0, \dots, K - 1$ , then train is coherent, otherwise it is referred to as incoherent. Moreover, if the target is absent (null hypothesis)  $A_k = 0$ ,  $k = 0, \dots, K - 1$ ;
- $n(t)$  is the **additive noise** component modeled as a complex circular zero-mean Gaussian random process with constant and known **PSD** within the receiver bandwidth.

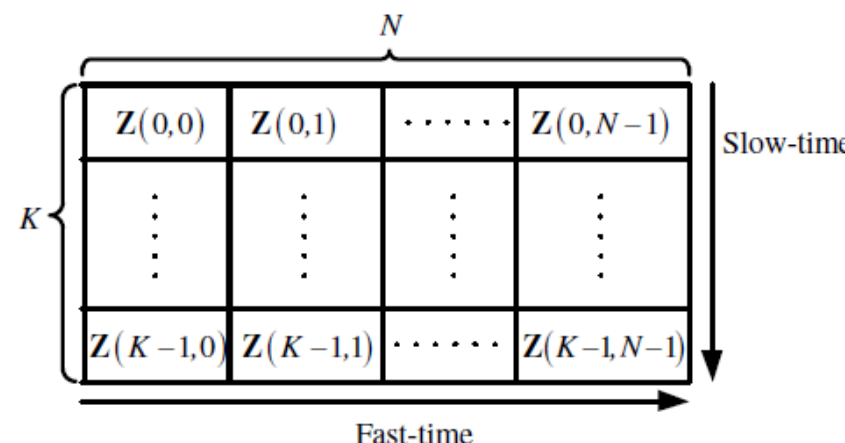


# PROBLEM FORMULATION

The received signal is filtered through a **sub-pulse** matched filter  $h(t) = u^*(-t)$  and sampled at the time instants  $iT_p + kT + \tau_0$ ,  $i = 0, \dots, N-1, k = 0, \dots, K-1$

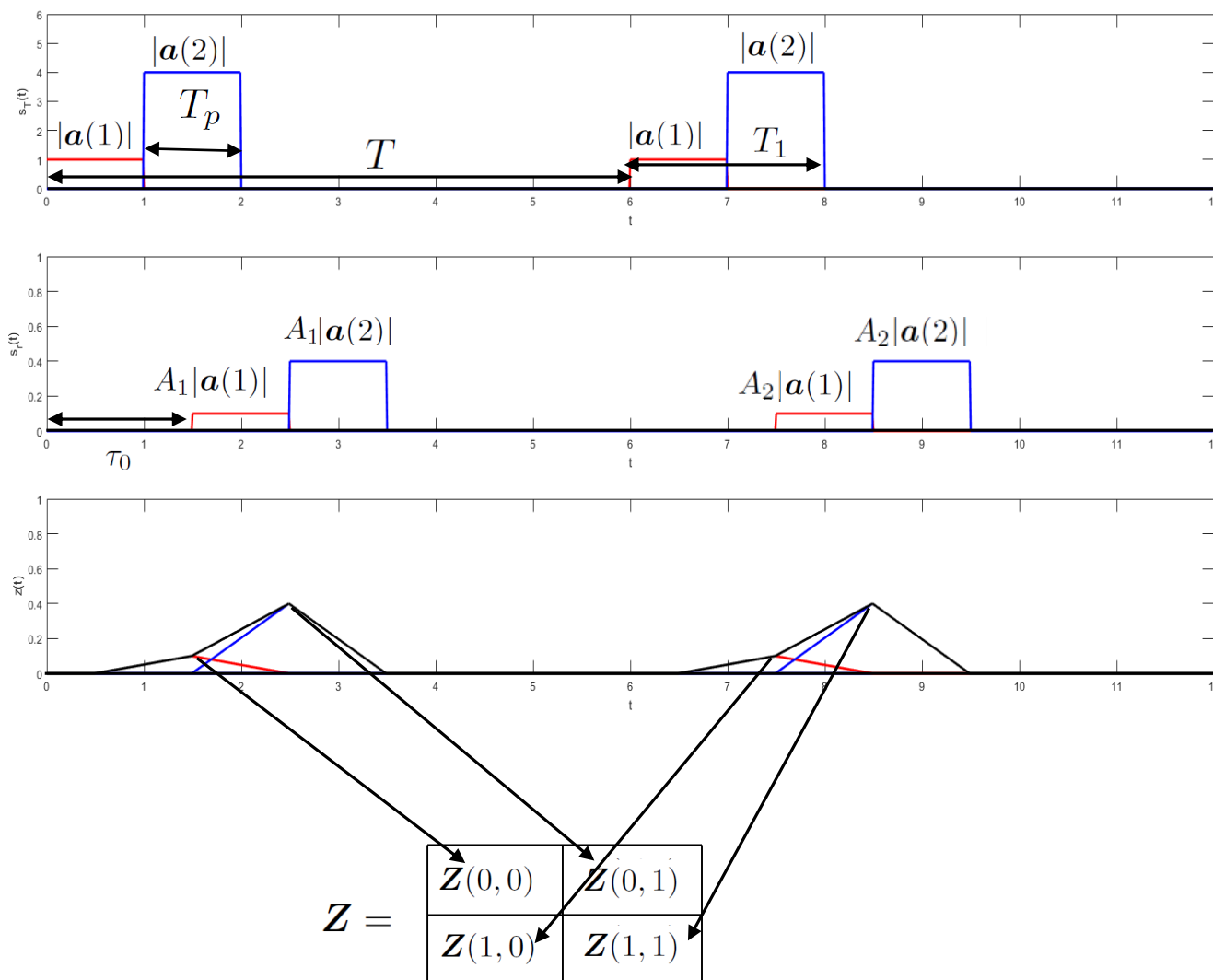


The samples  $Z(k,i)$ , from the **range cell under test**, are arranged into the fast-time/slow-time matrix  $Z$  of size  $K \times N$  whose columns contain the **slow-time samples** whereas its rows include those in **fast-time**.





# PROBLEM FORMULATION





# PROBLEM FORMULATION

Thus the **hypothesis test** under consideration can be formalized (under some very mild technical conditions) as

$$\begin{cases} H_0 : \mathbf{Z} = \mathbf{N}, \\ H_1 : \mathbf{Z} = \mathbf{Q}\mathbf{p}\mathbf{a}^\dagger + \mathbf{N}, \end{cases}$$

- $\mathbf{a} = [a(0), \dots, a(N-1)]^\dagger$  is the **code vector** assumed, without loss of generality, with unitary norm;
- $\mathbf{Q} = \text{diag}(\mathbf{q})$  with  $\mathbf{q} = [A_0 e^{j\theta_0}, \dots, A_{K-1} e^{j\theta_{K-1}}]^T$ ,  $\theta_k = \phi_k - 4\pi f_0 R_0 / c$ ;
- $\mathbf{p} = [1, e^{j2\pi f_d T}, \dots, e^{j2\pi f_d T(K-1)}]^T$  is the **temporal steering vector**;
- the entries of the  $K \times N$  matrix  $\mathbf{N}$ ,  $\mathbf{N}(k, i)$  for  $k = 0, \dots, K-1$ ,  $i = 0, \dots, N-1$ , are modeled as independent and identically distributed (i.i.d.) complex circular zero-mean **Gaussian random variables** with  $E[|\mathbf{N}(k, i)|^2] = \sigma^2$ , i.e.,  $\mathbf{N}(k, i)$  is  $CN(0, \sigma^2)$ .



# PROBLEM FORMULATION

In radar applications, the parameters  $A_k, e^{j\theta_k}$  (under the  $H_1$  hypothesis) are reasonably **unknown** and to circumvent this drawback two different approaches are usually exploited.

- a) modeling  $A_k, e^{j\theta_k}$  as **unknown deterministic** parameters
- b) a **Bayesian approach** which assigns suitable priors to the unknowns.

**Observation:** In the Bayesian case, the solution to the testing problem is often tied up to the specific priors whereas the deterministic and unknown parameter framework does not require any prior knowledge.

Based on this guideline the robust approach is considered.



# REDUCTION BY SUFFICIENCY

The considered testing problem is a **composite test** where the **simple hypothesis**  $H_0$  is tested versus the **composite alternative**  $H_1$ , with parameter vector  $\mathbf{q}$  and parameter space  $C^K$ .

**Procedure followed to solve it:**

- determine a **sufficient statistic** which summarizes all the information in the data about the parameters.
- After data reduction by sufficiency, which realizes a significant data compression, we synthesize the optimum Neyman-Pearson (**NP**) detector as the Likelihood Ratio Test (**LRT**) computed from the sufficient statistic.

Probability density function (**pdf**) under the  $H_1$  hypothesis

$$f_{\mathbf{Z}}(\mathbf{Z}|H_1) = \frac{1}{\pi^{NK} \sigma^{2NK}} \exp \left\{ -\frac{\text{Tr} \left[ (\mathbf{Z} - \mathbf{Q} \mathbf{p} \mathbf{a}^\dagger) (\mathbf{Z} - \mathbf{Q} \mathbf{p} \mathbf{a}^\dagger)^\dagger \right]}{\sigma^2} \right\}$$

The argument of the exponential can be recast as

$$-\frac{1}{\sigma^2} \text{Tr} (\mathbf{Z} \mathbf{Z}^\dagger) - \frac{1}{\sigma^2} \text{Tr} (\mathbf{Q} \mathbf{p} \mathbf{a}^\dagger \mathbf{a} \mathbf{p}^\dagger \mathbf{Q}^\dagger) + \frac{2}{\sigma^2} \text{Re} \left\{ \text{Tr} (\mathbf{Z} \mathbf{a} \mathbf{p}^\dagger \mathbf{Q}^\dagger) \right\}$$



# REDUCTION BY SUFFICIENCY

Based on the **Fisher-Neyman** factorization theorem and **minimality arguments** (details in Appendix) concerning regular exponential families, we can claim that

- 1) If the train is **coherent** then  $Q = Ae^{j\theta} I_K; Ae^{j\theta}$  is the sole unknown parameter; a minimal sufficient statistic is one-dimensional and coincides with

$$L = \text{Tr}(\mathbf{Z} \mathbf{a} p^\dagger)$$

- 2) If the train is **non-coherent** then  $A_k e^{j\theta_k}$  are the unknown parameters; a minimal sufficient statistic is  $K$ -dimensional and coincides with

$$\mathbf{L} = [\mathbf{Z}_{0,R} \mathbf{a} p^*(0), \dots, \mathbf{Z}_{K-1,R} \mathbf{a} p^*(K-1)]^T$$

where

$$\mathbf{Z} = [\mathbf{Z}_{0,R}^T, \mathbf{Z}_{1,R}^T, \dots, \mathbf{Z}_{K-1,R}^T]^T$$



# REDUCTION BY SUFFICIENCY

Important Remark:

$$\mathbf{L} = [\mathbf{Z}_{0,R} \mathbf{a} \mathbf{p}^*(0), \dots, \mathbf{Z}_{K-1,R} \mathbf{a} \mathbf{p}^*(K-1)]^T$$

represents a **sufficient statistic** also for the coherent train detection problem; however in this last case it is not **minimal**.

Its computation requires a linear filtering procedure matched to the **radar code** namely, in radar jargon, a **pulse compression**.

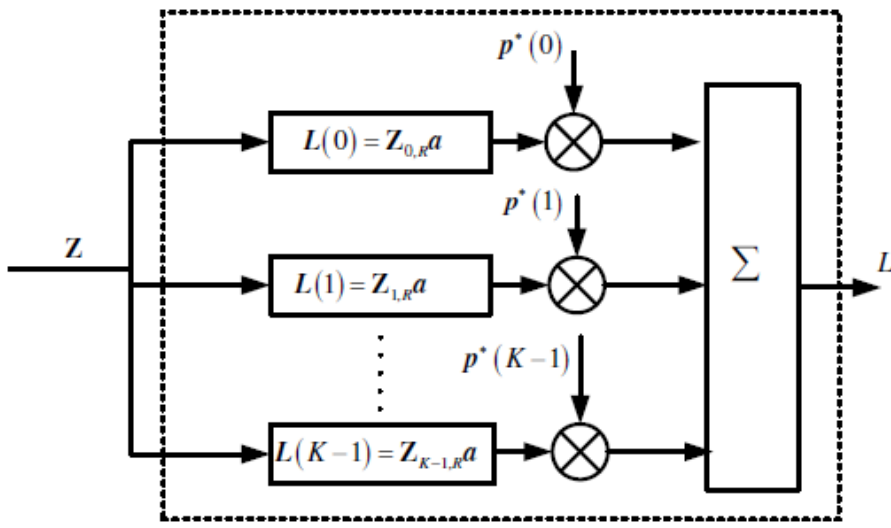
Besides, with reference to the coherent case, since

$$\text{Tr}[(\mathbf{Z}\mathbf{a}) \mathbf{p}^\dagger] = \text{Tr}[(\mathbf{p}^\dagger \mathbf{Z}) \mathbf{a}],$$

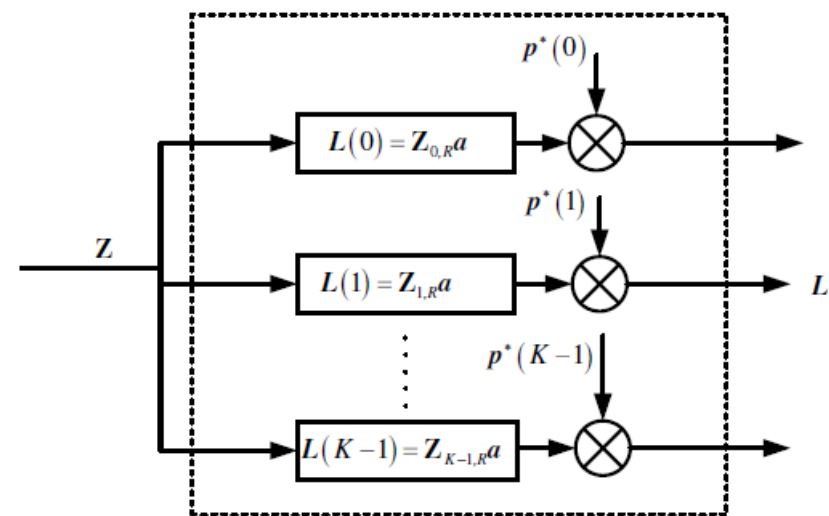
from a theoretical point of view it is possible to decide arbitrarily which processing between fast-time (**pulse compression**) and slow-time (**Doppler processing**) to implement first.



# REDUCTION BY SUFFICIENCY



(a)



(b)

Block schemes for the computation of  $L$  (a) and  $L$  (b).

The main difference relies on the final coherent integration required for  $L$ .

# OPTIMUM NEYMAN-PEARSON DETECTOR AND EXISTENCE OF THE UMP TEST



The scope is twofold:

1. firstly to synthesize the **optimum detector**, according to the Neyman-Pearson criterion for the considered hypotheses testing problem;
2. secondly, due to the composite nature of the  $H_1$  hypothesis, to ascertain the existence of a Uniformly Most Powerful (UMP) test.

The optimum detector, which maximizes the detection performance for a given false alarm probability, is the **LRT** computed from the sufficient statistic.

In order to proceed with the synthesis, let us distinguish between the **coherent** and **non-coherent** cases.



## COHERENT CASE

The LRT detector from the sufficient statistic can be expressed as

$$\frac{f_L(L|H_1)}{f_L(L|H_0)} \stackrel{H_1}{\underset{H_0}{\gtrless}} \gamma$$

where  $f_L(L|H_0)$  and  $f_L(L|H_1)$  are the likelihood functions of the sufficient statistic under the  $H_0$  and the  $H_1$  hypothesis respectively.

Observing that  $L|H_0$  is  $CN(0, K\sigma^2)$  and  $L|H_1$  is  $CN(KAe^{j\theta}, K\sigma^2)$ , the NP receiver can be written as

$$\frac{f_L(L|H_1)}{f_L(L|H_0)} = \exp \left\{ -\frac{|L - KAe^{j\theta}|^2 - |L|^2}{K\sigma^2} \right\} \stackrel{H_1}{\underset{H_0}{\gtrless}} \gamma$$

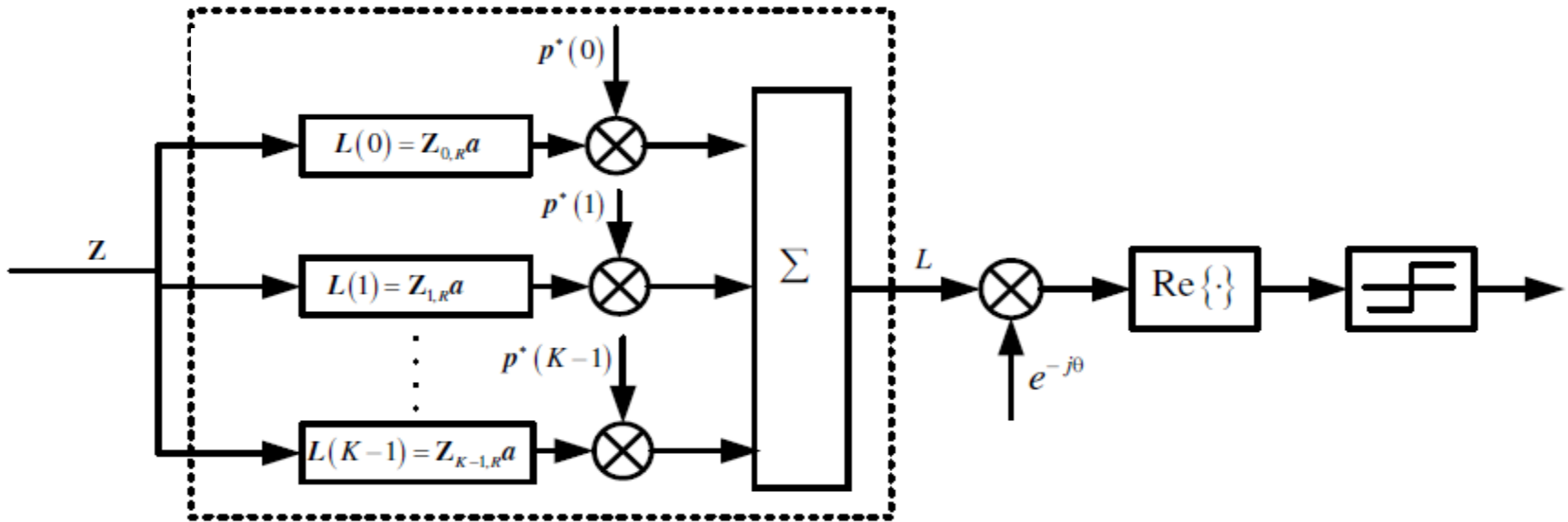
After some algebraic manipulations, taking the logarithm and absorbing inessential terms into the detection threshold, we get

$$\text{Re} \left\{ e^{-j\theta} L \right\} = \text{Re} \left\{ e^{-j\theta} p^\dagger(\mathbf{Z}\mathbf{a}) \right\} \stackrel{H_1}{\underset{H_0}{\gtrless}} \gamma$$

where  $\gamma$  is a suitable modification of the original detection threshold.



# COHERENT CASE



Block scheme of the NP detector for the coherent train.

It is not **implementable** since it requires the exact knowledge of the phase; otherwise stated the **UMP test does not exist**.

Nevertheless, the optimum detector is still important as it provides an **upper-bound** to the performance of any practically feasible detection schemes.



## NON-COHERENT CASE

The LRT from the sufficient statistic  $\mathbf{L}$  can be expressed as

$$\frac{f_{\mathbf{L}}(\mathbf{L}|H_1)}{f_{\mathbf{L}}(\mathbf{L}|H_0)} \stackrel{H_1}{\underset{H_0}{\gtrless}} \gamma$$

where the entries of  $\mathbf{L}$  are independent complex circular Gaussian random variables:

$$H_0 \quad Z_{k,R} \mathbf{a} \mathbf{p}^*(k) \sim \mathcal{CN}(0, \sigma^2),$$

$$H_1 \quad Z_{k,R} \mathbf{a} \mathbf{p}^*(k) \sim \mathcal{CN}(A_k e^{j\theta_k}, \sigma^2).$$

The NP detector can be recast as

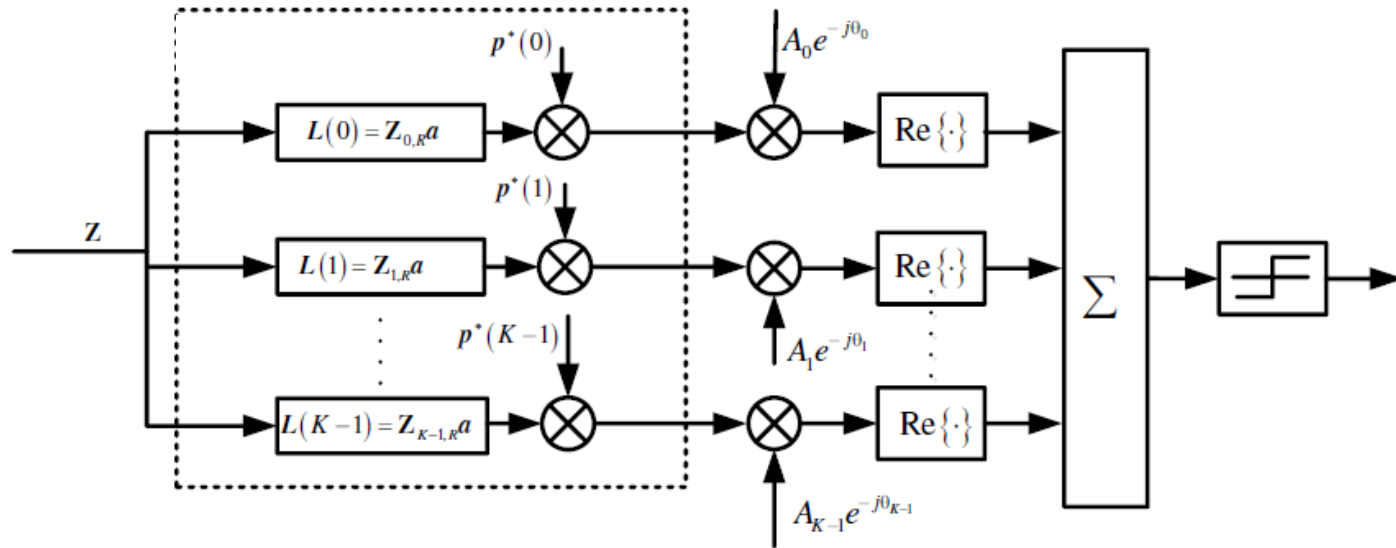
$$\frac{f_{\mathbf{L}}(\mathbf{L}|H_1)}{f_{\mathbf{L}}(\mathbf{L}|H_0)} = \exp \left\{ -\frac{\sum_{k=0}^{K-1} |L(k) - A_k e^{j\theta_k}|^2 - \mathbf{L}^\dagger \mathbf{L}}{\sigma^2} \right\} \stackrel{H_1}{\underset{H_0}{\gtrless}} \gamma,$$

which can be shown equivalent to

$$\sum_{k=0}^{K-1} \operatorname{Re} \{ A_k e^{-j\theta_k} L(k) \} = \sum_{k=0}^{K-1} \operatorname{Re} \{ A_k e^{-j\theta_k} \mathbf{p}^*(k) \mathbf{Z}_{k,R} \mathbf{a} \} \stackrel{H_1}{\underset{H_0}{\gtrless}} \gamma$$



# NON-COHERENT CASE



First of all, **fast-time processing** is performed. Then the  $K$  outputs (corresponding to different pulses) are:

- 1) compensated for the **phase terms** induced by the lack of coherence;
- 2) weighted according to the **useful signal strength** on that specific pulse.

Finally, the **real parts** of the aforementioned quantities are summed and compared with the detection threshold.

# GENERALIZED LIKELIHOOD RATIO TEST (GLRT) DESIGN: MOTIVATION



For both the coherent and non-coherent cases,

**the NP detector is not UMP**

and, hence,

**it is not practically implementable.**

To circumvent this drawback, we resort to a robust design framework based on the GLRT which is tantamount to substituting the **Maximum Likelihood Estimates** (MLEs) of the unknown parameters in place of their exact values.



## GLRT DESIGN: COHERENT CASE

We write the **GLRT** as

$$\frac{\max_{A,\theta} f_L(L|H_1)}{f_L(L|H_0)} \stackrel{H_1}{\underset{H_0}{\gtrless}} \gamma$$

Applying the logarithm to both the sides, the **GLRT** reduces to

$$\max_{A,\theta} \ln f_L(L|H_1) - \ln f_L(L|H_0) \stackrel{H_1}{\underset{H_0}{\gtrless}} \ln \gamma$$

The left hand side of the above equation can be computed as

$$\max_{A,\theta} \ln f_L(L|H_1) - \ln f_L(L|H_0) = \frac{|L|^2}{K\sigma^2} - \min_{A,\theta} \frac{(L - K A e^{j\theta})^\dagger (L - K A e^{j\theta})}{K\sigma^2} \leq \frac{|L|^2}{K\sigma^2}$$

with equality if and only if  $A e^{j\theta} = L / K$ .

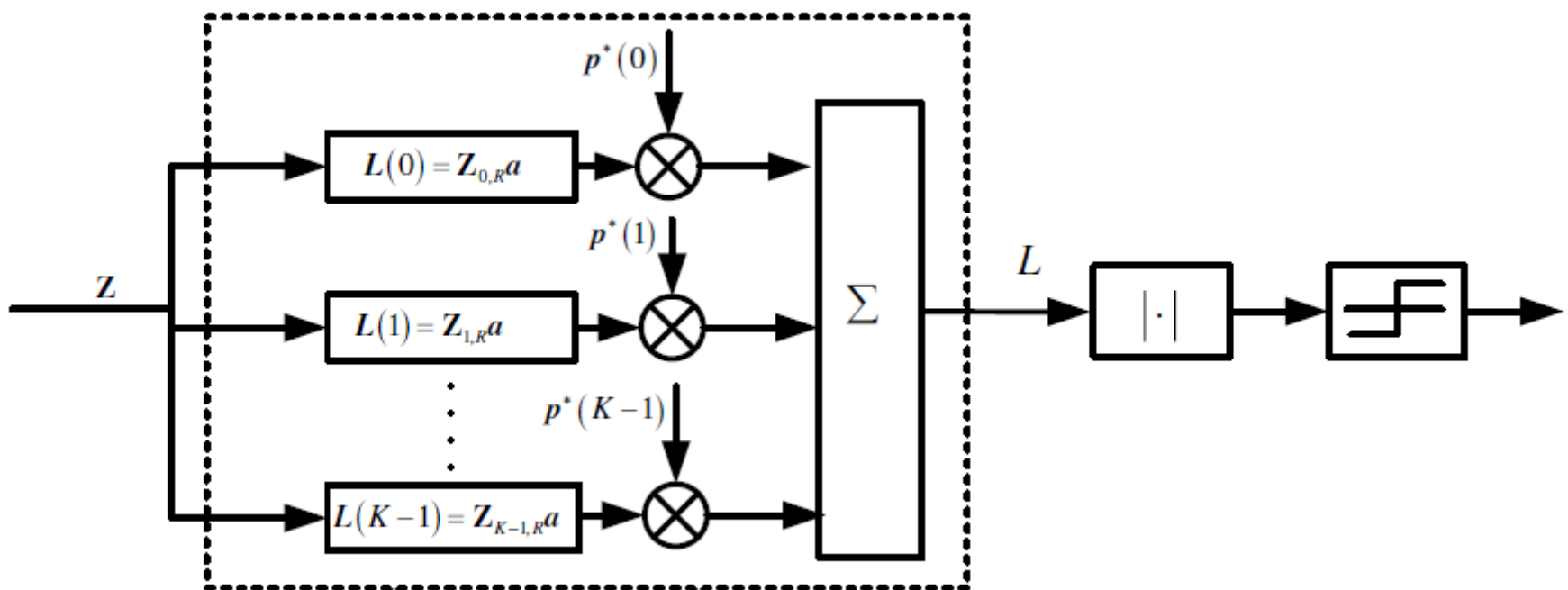
Hence, the **GLRT** for the coherent case can be recast as

$$|p^\dagger(Za)| \stackrel{H_1}{\underset{H_0}{\gtrless}} \gamma$$



# GLRT DESIGN: COHERENT CASE

After the **coherent sum** performed to compute  $L$ , the **magnitude** of the resulting complex number is **compared** with a detection threshold.





## GLRT DESIGN: COHERENT CASE

Further **insights** in the required processing can be obtained writing the decision statistic as

$$\left| \sum_{k=0}^{K-1} (\mathbf{Z}_{k,R} \mathbf{a}) e^{-j2\pi k f_d T} \right|$$

namely as the Discrete Time Fourier Transform (**DTFT**) of the fast-time samples after pulse compression.

This expression explicitly highlights that with the same range processing (namely exploiting the same pulse compression outputs), it is possible to test all the Doppler cells just changing the value of  $f_d$ .

An **important remark** is now in order: **GLRT** detector coincides with the NP test obtained modeling the target phase as a uniformly distributed random variable within the interval  $[0, 2\pi[$ .



# GLRT DESIGN: NON-COHERENT CASE

We have to distinguish between two different **situations**:

1. The **amplitudes** of the returns are equal, e.g.,  $A_k = A$ ,  $k = 0, \dots, K - 1$ ;
2. The **amplitudes**  $A_k$  represent  $K$  unknown parameters without any known a-priori relationship.

## Case 1, Incoherent Pulse Train with one and the same Amplitude:

The **GLRT** is

$$\max_{A, \theta_0, \dots, \theta_{K-1}} \frac{f_L(L|H_1)}{f_L(L|H_0)} \stackrel{H_1}{\gtrless} \gamma$$

or equivalently,

$$-\min_A \sum_{k=0}^{K-1} \left[ \min_{\theta_k} |L(k) - Ae^{j\theta_k}|^2 - |L(k)|^2 \right] \stackrel{H_1}{\gtrless} \gamma$$



## GLRT DESIGN: NON-COHERENT CASE

To perform the optimizations over  $\theta_k$ , we observe that the reverse triangular inequality implies

$$|\mathbf{L}(k) - Ae^{j\theta_k}|^2 \geq ||\mathbf{L}(k)| - A|^2, \quad k = 0, \dots, K-1$$

with equality if  $\theta_k = \angle \mathbf{L}(k)$ . As a consequence, the GLRT becomes equivalent to

$$-\min_A \sum_{k=0}^{K-1} [A^2 - 2A|\mathbf{L}(k)|] \stackrel{H_1}{\underset{H_0}{\gtrless}} \gamma$$

Hence, optimizing over  $A$ , the **GLRT** can be finally expressed as

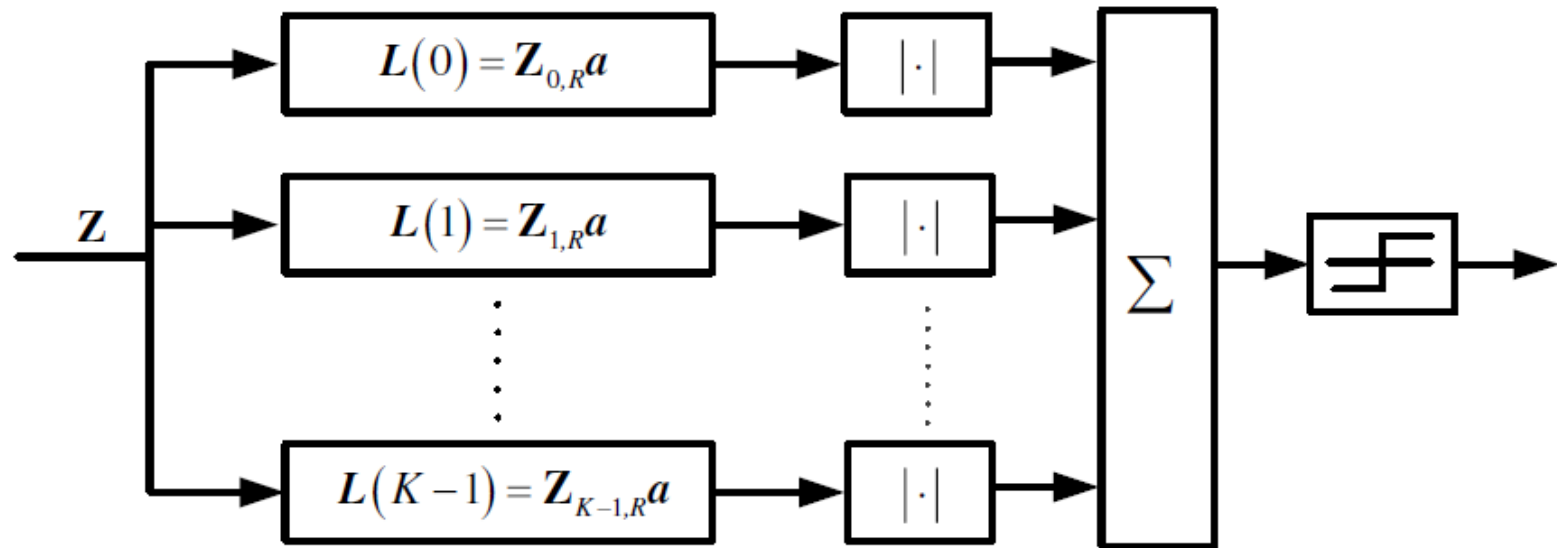
$$\sum_{k=0}^{K-1} |\mathbf{L}(k)| \stackrel{H_1}{\underset{H_0}{\gtrless}} \gamma$$

and is usually referred to as **linear non-coherent integrator**.



# GLRT DESIGN: NON-COHERENT CASE

Block scheme of the linear non-coherent detector.



**Remark:** The final multipliers involved in the computation of the sufficient statistic  $L$  are omitted because any phase information is lost due to the presence of the modulus operation, i.e.  $|L(k)| = |Z_{k,R}a|$ .

This also justifies why practically implementable non-coherent processing is unable to provide any information on the actual target Doppler.



## GLRT DESIGN: NON-COHERENT CASE

### Case 2, Incoherent Pulse Train with Different Amplitudes:

The GLRT is given by

$$\max_{A_0, \dots, A_{K-1}, \theta_0, \dots, \theta_{K-1}} \frac{f_L(L|H_1)}{f_L(L|H_0)} \stackrel{H_1}{\gtrless} \gamma$$

or equivalently,

$$\sum_{k=0}^{K-1} \left[ \min_{A_k, \theta_k} |L(k) - A_k e^{j\theta_k}|^2 - |L(k)|^2 \right] \stackrel{H_1}{\gtrless} \gamma$$

Optimizations over  $A_k$  and  $\theta_k$  yield  $A_k = |L(k)|$  and  $\theta_k = \angle L(k)$  for  $k = 0, \dots, K-1$ .

The GLRT is thus equivalent to

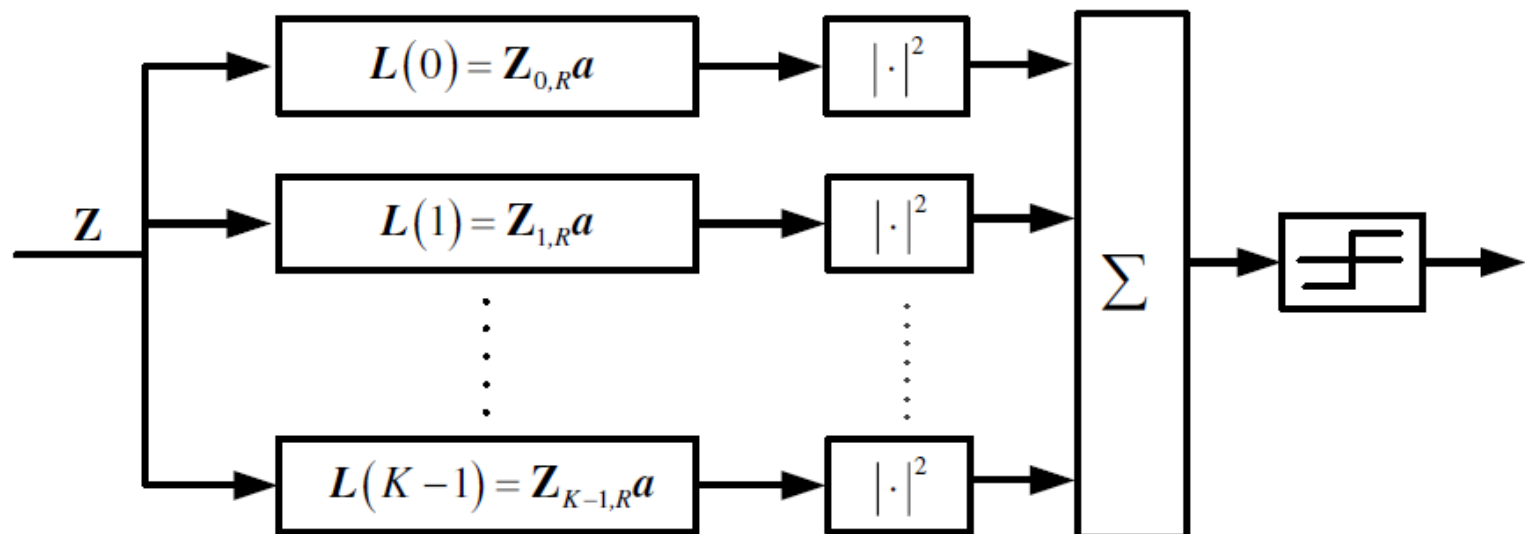
$$\sum_{k=0}^{K-1} |L(k)|^2 \stackrel{H_1}{\gtrless} \gamma$$

which is usually referred to as **square law non-coherent integrator**.



# GLRT DESIGN: NON-COHERENT CASE

Block scheme of the square law non-coherent integrator.





# GLRT DESIGN: CONSIDERATIONS

- a) The linear non-coherent integrator can be also obtained as the high Signal-to-Noise Ratio (SNR) approximation of the NP receiver designed for  $A_k = A$ ,  $k = 0, \dots, K - 1$ , and i.i.d. target phases modeled as uniformly distributed within  $[0, 2\pi[$ .
- b) Under the same assumptions on the amplitudes and phases, the square law non-coherent integrator can be interpreted as the approximation of the NP receiver in the low SNR regime.
- c) The square law non-coherent integrator is the optimum NP test designed assuming i.i.d. Rayleigh distributed amplitudes  $A_k$ ,  $k = 0, \dots, K - 1$ , and i.i.d. target phases (statistically independent from the amplitudes) uniformly distributed within  $[0, 2\pi[$ .
- d) While a Bayesian receiver is based on the assignment of some priors for the unknown parameters, the GLRT does not require this knowledge. As a result, the former is tied up to the specific parameter fluctuation law whereas the latter **is one and the same** independently of the considered priors and their parameters.



## GLRT DESIGN: CONSIDERATIONS

- e) For the **coherent** case, assuming a uniformly distributed phase within  $[0, 2\pi[$ , the resulting Bayesian detector is one and the same independent of the amplitude prior. Moreover it also coincides with the **GLRT**.
- f) For the non-coherent case, assuming statistically independent and uniformly distributed phases, the **Bayesian approach** leads to detectors tied up to the fluctuation laws of the return amplitudes (specifically on their joint probability density function). As a consequence mismatches between the design and actual fluctuation laws may lead to performance degradations. On the contrary the **GLRT** is a universal receiver.
- g) In general the **GLRT** is not statistically equivalent to the **Bayesian detector** (an exception is the i.i.d. Rayleigh fluctuating amplitudes case).



# PERFORMANCE ANALYSIS

Analytic expressions for the **False Alarm Probability** ( $P_{FA}$ ) and **Detection Probability** ( $P_D$ ) are provided except for the linear non-coherent integrator whose performance is obtained via Monte Carlo simulations due to the lack of easily manageable analytic formulas.

**Coherent case:** the **GLRT** performance is compared with the optimum benchmark curve ensured by the **clairvoyant structure** and the effect of the coherent integration gain is assessed.

**Non-coherent case:** a performance comparison among the **linear**, **square-law**, and **optimum non-coherent integration** is conducted. Finally, the effect of non-coherent integration is discussed.



# PERFORMANCE ANALYSIS: COHERENT CASE

Let us focus on the NP detector for coherent pulse trains, and denote by

$$l_1 = \operatorname{Re} \left\{ e^{-j\theta} \mathbf{p}^\dagger \mathbf{Z} \mathbf{a} \right\}$$

Under the  $H_1$  hypothesis,  $e^{-j\theta} \mathbf{p}^\dagger \mathbf{Z} \mathbf{a} \sim \mathcal{CN}(KA, K\sigma^2)$

Hence,  $l_1$  is a real Gaussian random variable with mean  $\mu_{l_1} = KA$  and variance  $\sigma_{l_1}^2 = K\sigma^2/2$ , namely

$$f_{l_1}(t|H_1) = \frac{1}{\sqrt{2\pi}\sigma_{l_1}} \exp\left(-\frac{(t - \mu_{l_1})^2}{2\sigma_{l_1}^2}\right)$$

This implies that  $P_D$  can be obtained as

$$P_D = \int_{\gamma}^{\infty} f_{l_1}(t|H_1) dx = Q\left(\frac{\gamma - KA}{\sqrt{K\sigma^2/2}}\right)$$

where  $Q(\cdot)$  is the Q-function 
$$Q(x) = \frac{1}{\sqrt{2\pi}} \int_x^{\infty} \exp\left(-\frac{t^2}{2}\right) dt$$



# PERFORMANCE ANALYSIS: COHERENT CASE

$P_{FA}$  can be obtained setting  $A = 0$  in the  $P_D$  expression, i.e.,

$$P_{FA} = Q\left(\frac{\gamma}{\sqrt{K\sigma^2/2}}\right)$$

Using the **inverse Q-function**, the Receiver Operating Characteristic (**ROC**) can be computed as

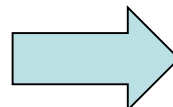
$$P_D = Q\left(Q^{-1}(P_{FA}) - \sqrt{2K\text{SNR}}\right)$$

where **SNR** per pulse is given by  $\text{SNR} = \frac{A^2}{\sigma^2}$



# PERFORMANCE ANALYSIS: COHERENT CASE

GLRT for the coherent case and denote by  $g_1 = |p^\dagger Z a|$

Under the  $H_1$ ,  $p^\dagger Z a \sim \mathcal{CN}(KAe^{j\theta}, K\sigma^2)$    $g_1$  is Rician distributed

$$f_{g_1}(z|H_1) = \frac{2z}{K\sigma^2} \exp\left(-\frac{z^2 + K^2 A^2}{K\sigma^2}\right) I_0\left(\frac{2zA}{\sigma^2}\right) U(z) \quad \text{where} \quad U(z) = \begin{cases} 1, & z \geq 0, \\ 0, & z < 0, \end{cases}$$

and  $I_\nu(x)$  is the modified Bessel function of the first kind and order  $\nu$ ,

$$I_\nu(x) = \sum_{m=0}^{\infty} \frac{1}{m! \Gamma(m + \nu + 1)} \left(\frac{x}{2}\right)^{2m+\nu}$$

It follows that  $P_D$  can be obtained as  $P_D = \int_{\gamma}^{\infty} f_{g_1}(z|H_1) dz = Q_1\left(\sqrt{\frac{2KA^2}{\sigma^2}}, \sqrt{\frac{2\gamma^2}{K\sigma^2}}\right)$

$$Q_m(a, b) = \int_b^{\infty} \frac{x^m}{a^{m-1}} \exp\left\{-\frac{x^2 + a^2}{2}\right\} I_{m-1}(ax) dx$$

Generalized Marcum function of order  $m$



# PERFORMANCE ANALYSIS: COHERENT CASE

Under the  $H_0$ ,  $g_1$  is Rayleigh distributed with parameter  $\sigma_{g1}^2 = K \sigma^2 / 2$ , i.e.,

$$f_{g1}(z|H_0) = \frac{2z}{K\sigma^2} \exp\left(-\frac{z^2}{K\sigma^2}\right) U(z)$$

Thus,  $P_{FA}$  can be computed as

$$P_{FA} = \exp\left(-\frac{\gamma^2}{K\sigma^2}\right)$$

whereas the ROC is

$$P_D = Q_1\left(\sqrt{2K\text{SNR}}, \sqrt{-2 \ln P_{FA}}\right)$$

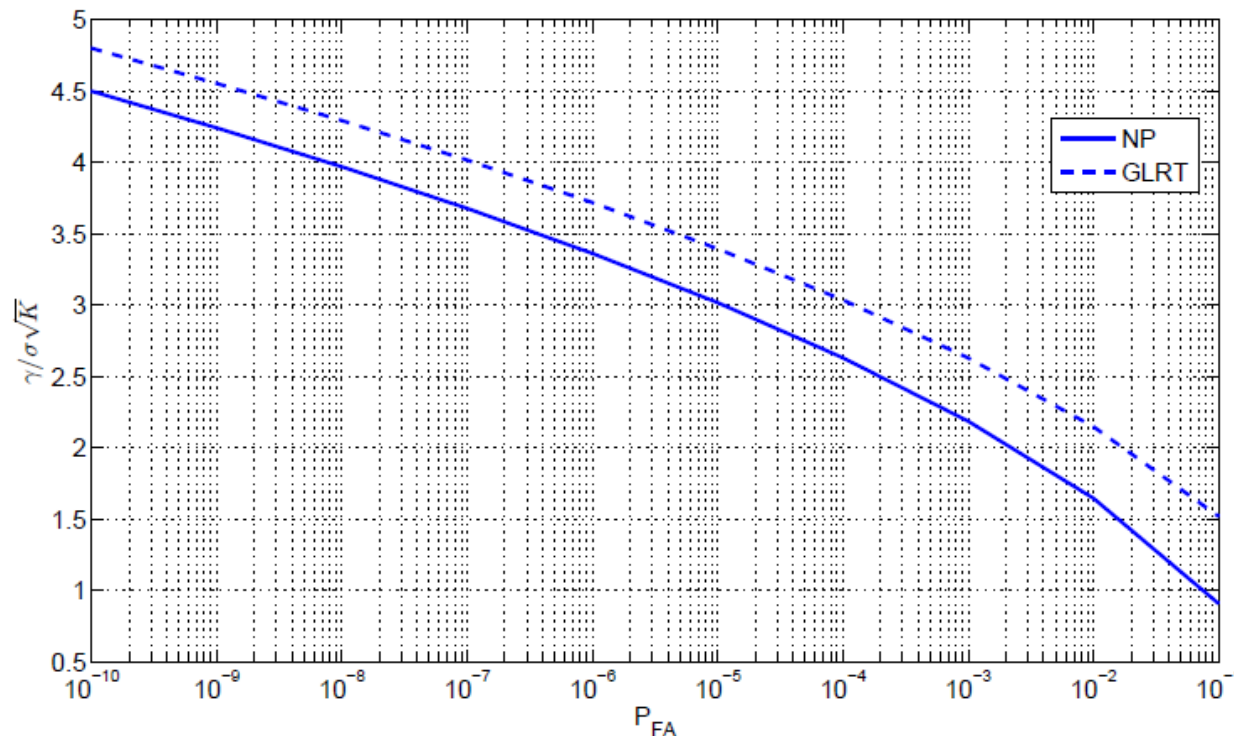
ROC expression clearly highlights the effect of coherent integration. Precisely, the **Coherent Equivalent SNR (SNR<sub>ceq</sub>)** after coherent integration can be obtained multiplying the single pulse SNR and the number of transmitted pulses, namely,

$$\text{SNR}_{\text{ceq}} = K \text{SNR}.$$



# PERFORMANCE ANALYSIS: COHERENT CASE

Normalized detection thresholds  $\gamma / (\sigma K^{1/2})$  are plotted versus  $P_{FA}$ .

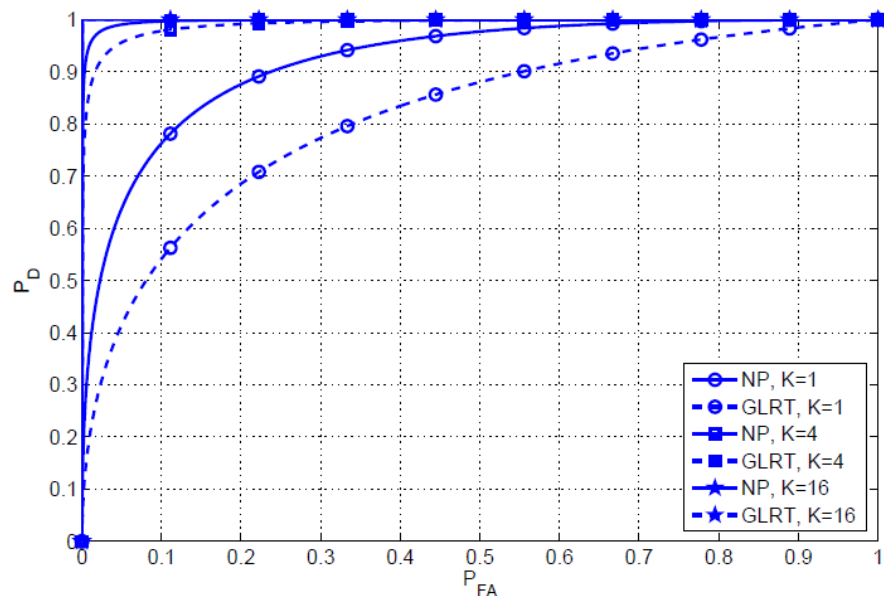


Being  $P_{FA}$  versus the normalized threshold a Complementary Cumulative Distribution Function (CCDF), the larger  $P_{FA}$ , the lower the detection threshold. Moreover, the NP receiver requires a lower normalized threshold than the GLRT.

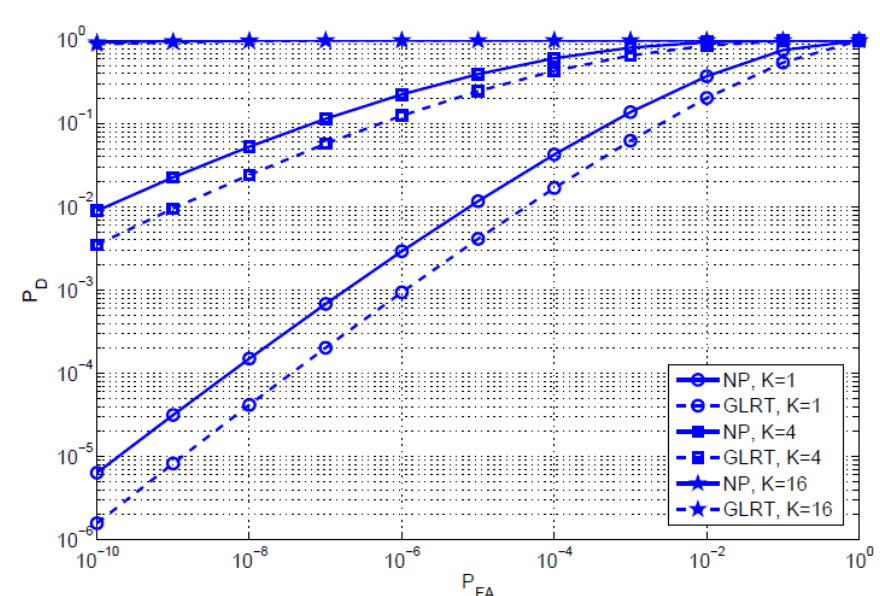
# PERFORMANCE ANALYSIS: COHERENT CASE



Figures (a) and (b), show the **ROC** of the **NP** receiver and **GLRT** for SNR = 3dB and  $K$  in  $\{1, 4, 16\}$  using two different scales: a linear scale, in figure (a), and a logarithmic scale, in figure (b), necessary to emphasize the  $P_D$  behavior for low  $P_{FA}$  values.



(a)



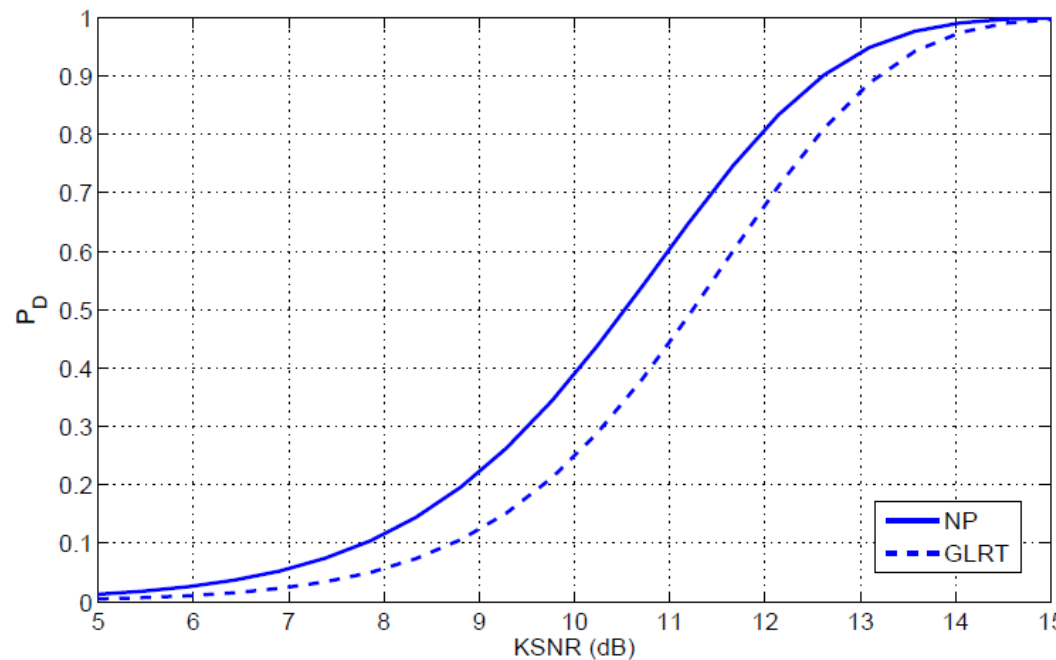
(b)

The larger  $P_{FA}$  and  $K$ , the higher  $P_D$ . Specifically, with reference to the **NP** receiver,  $P_D$ s are approximately 0.04, 0.6, and 1 at  $P_{FA} = 10^{-4}$  for  $K = 1, 4$ , and 16, respectively. As to the **GLRT**, they are approximately 0.01, 0.4, and 1, respectively.



# PERFORMANCE ANALYSIS: COHERENT CASE

$P_D$  of the GLRT and the clairvoyant structure versus  $K$  SNR for  $P_{FA} = 10^{-6}$ .



The GLRT requires about 0.6 dB higher  $K$  SNR than the NP detector at  $P_D = 0.9$  and about 0.7 dB at  $P_D = 0.5$ .

It is worth mentioning the universality of the representation in the figure. It completely characterizes the performance of the considered coherent detectors for any values of  $K$  and single pulse SNR.



# PERFORMANCE ANALYSIS: NON-COHERENT CASE

Let us focus on the **clairvoyant structure**

$$\sum_{k=0}^{K-1} \operatorname{Re} \left\{ A_k e^{-j\theta_k} \mathbf{L}(k) \right\} = \sum_{k=0}^{K-1} \operatorname{Re} \left\{ A_k e^{-j\theta_k} \mathbf{p}^*(k) \mathbf{Z}_{k,R} \mathbf{a} \right\} \stackrel{H_1}{\underset{H_0}{\gtrless}} \gamma$$

and denote by

$$l_2 = \sum_{k=0}^{K-1} \operatorname{Re} \left\{ A_k e^{-j\theta_k} \mathbf{p}^*(k) \mathbf{Z}_{k,R} \mathbf{a} \right\}$$

the decision statistic. Under  $H_1$

$$\sum_{k=0}^{K-1} A_k e^{-j\theta_k} \mathbf{p}^*(k) \mathbf{Z}_{k,R} \mathbf{a} \sim \mathcal{CN} \left( \sum_{k=0}^{K-1} A_k^2, \sum_{k=0}^{K-1} A_k^2 \sigma^2 \right)$$

Thus,  $l_2$  follows a real **Gaussian** distribution with average  $\mu_{l_2} = \sum_{k=0}^{K-1} A_k^2$  and variance  $\sigma_{l_2}^2 = \sum_{k=0}^{K-1} A_k^2 \sigma^2 / 2$ . This implies that  $P_D$  can be obtained as

$$P_D = Q \left( \frac{\gamma - \sum_{k=0}^{K-1} A_k^2}{\sqrt{\sum_{k=0}^{K-1} A_k^2 \sigma^2 / 2}} \right).$$



# PERFORMANCE ANALYSIS: NON-COHERENT CASE

Under  $H_0$ ,  $I_2$  follows a real zero-mean Gaussian distribution with variance  $\sigma_{I_2}^2 = \sum_{k=0}^{K-1} A_k^2 \sigma^2 / 2$ . Hence,  $P_{FA}$  can be computed as

$$P_{FA} = Q\left(\frac{\gamma}{\sqrt{\sum_{k=0}^{K-1} A_k^2 \sigma^2 / 2}}\right)$$

Note that if  $A_k = A$ ,  $k = 0, \dots, K-1$ , the NP detector for the non-coherent case reduces to

$$\sum_{k=0}^{K-1} \operatorname{Re} \left\{ e^{-j\theta_k} L(k) \right\} \stackrel{H_1}{\gtrless} \stackrel{H_0}{\lesssim} \gamma$$

whose  $P_D$  and  $P_{FA}$  are respectively the same as those obtained in the coherent case.

Using the inverse Q-function and the obtained  $P_{FA}$ , the ROC can be recast as

$$P_D = Q\left(Q^{-1}(P_{FA}) - \sqrt{2K\text{SNR}_{\text{eq}}}\right)$$

where  $\text{SNR}_{\text{eq}}$  denotes the equivalent SNR per pulse, defined as  $\text{SNR}_{\text{eq}} = \frac{1}{K} \sum_{k=0}^{K-1} \frac{A_k^2}{\sigma^2}$ .



# PERFORMANCE ANALYSIS: NON-COHERENT CASE

The ROC for **coherent** and **non-coherent** case reveals that they share the same functional expression with the only difference due to the presence of  $\text{SNR}_{\text{eq}}$  in place of the single pulse SNR.

The **optimum** non-coherent processing still provides a coherent integration gain. As to the **GLRT** of case 1 (linear integrator), there are no known easily manageable analytical expressions for  $P_{FA}$  and  $P_D$ .

Hence, in the following, it is only considered the analytic performance evaluation of the **square law detector**, whereas Monte Carlo simulations are used to analyze the behavior of the linear detector for which it is considered  $A_k = A$  for  $k = 0, \dots, K - 1$ .

To this end, denote by  $g_2 = \sum_{k=0}^{K-1} |L(k)|^2$  and define  $r = g_2 / \sigma^2$  as the normalized **decision statistic**.



# PERFORMANCE ANALYSIS: NON-COHERENT CASE

Under  $H_1$ ,  $r$  is a complex non-central chi-square random variable with  $K$  Degrees of Freedom (DOF) and non-centrality parameter  $\chi_K = \sum_{k=0}^{K-1} A_k^2 / \sigma^2$  i.e.,

$$f_r(r|H_1) = \left( \frac{r}{\chi_K} \right)^{(K-1)/2} e^{-r-\chi_K} I_{K-1}(2\sqrt{r\chi_K}) U(r)$$

As a consequence,  $P_D$  can be obtained as

$$\begin{aligned} P_D &= P\{g_2 \geq \gamma|H_1\} = P\{g_2/\sigma^2 \geq \gamma/\sigma^2|H_1\} = Q_K \left( \sqrt{2 \sum_{k=0}^{K-1} A_k^2 / \sigma^2}, \sqrt{2\gamma/\sigma^2} \right) \\ &= Q_K \left( \sqrt{2K\text{SNR}_{\text{eq}}}, \sqrt{2\gamma/\sigma^2} \right) \end{aligned}$$

This last expression clearly shows the lack of a coherent integration gain because the functional relationship between  $P_D$  and the two arguments in the generalized Marcum function depends on the number of pulses  $K$ .

# PERFORMANCE ANALYSIS: NON-COHERENT CASE



Under  $H_0$ ,  $r$  is distributed as a **complex central chi-square** random variable with  $K$  DOF, namely its pdf is given by

$$f_r(r|H_0) = \frac{r^{K-1}}{(K-1)!} e^{-r} U(r)$$

Hence,  $P_{FA}$  can be computed as

$$P_{FA} = P\{g_2 \geq \gamma|H_0\} = P\{g_2/\sigma^2 \geq \gamma/\sigma^2|H_0\} = \frac{1}{\Gamma(K)} \Gamma_{inc}(K, \gamma/\sigma^2)$$

where  $\Gamma_{inc}(n, x)$  denotes the incomplete Gamma function, i.e.,

$$\Gamma_{inc}(n, x) = \int_x^\infty t^{n-1} \exp(-t) dt$$

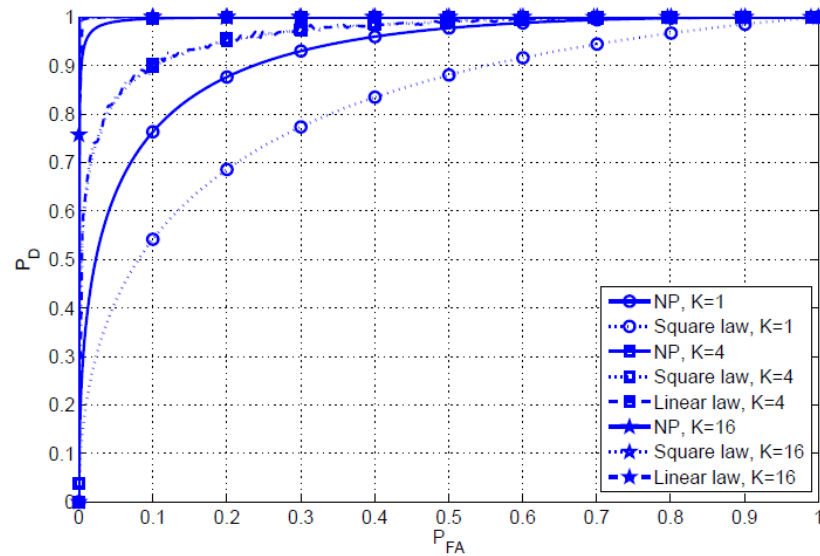
Moreover,  $P_{FA}$  can be rewritten as a finite summation, i.e.,

$$P_{FA} = \exp\left(-\frac{\gamma}{\sigma^2}\right) \sum_{k=0}^{K-1} \frac{1}{k!} \left(\frac{\gamma}{\sigma^2}\right)^k$$

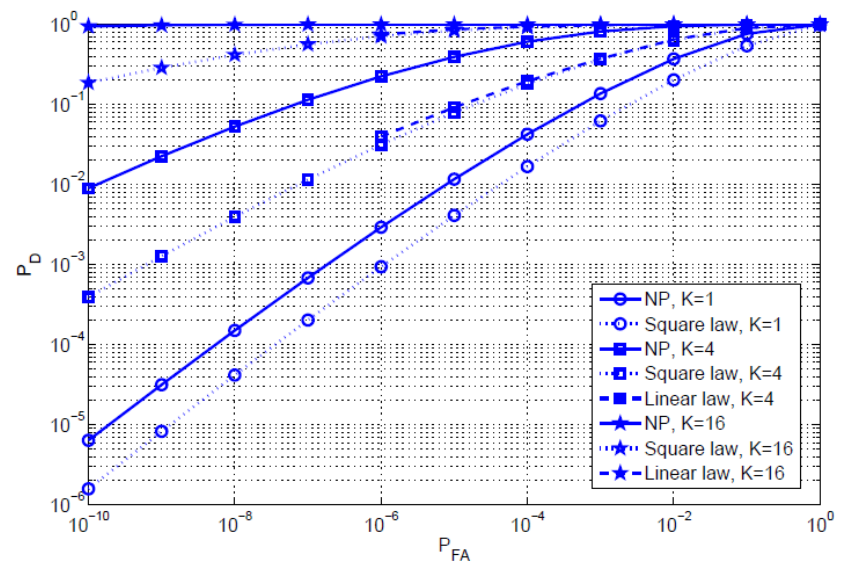


# PERFORMANCE ANALYSIS: NON-COHERENT CASE

ROCs of the NP detector of the linear law detector (exploiting Monte Carlo simulations), and of the square law detector.



(a)



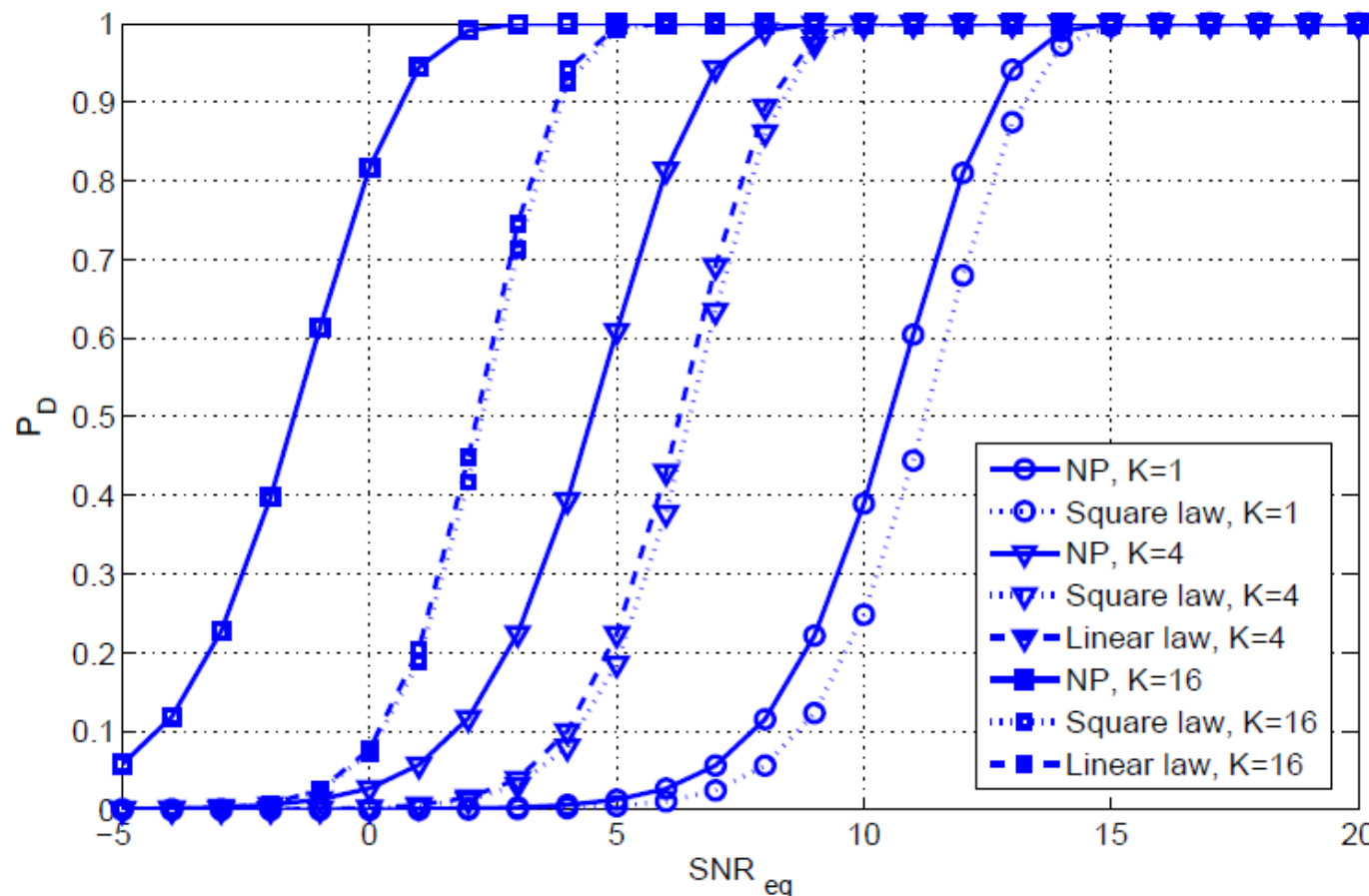
(b)

The performance gaps between the NP receiver and GLRTs become larger and larger as  $K$  increases. This can be explained observing that the clairvoyant structure coherently integrates the available samples whereas the GLRTs, neglecting the phase information on each pulse, only performs a non-coherent integration.



# PERFORMANCE ANALYSIS: NON-COHERENT CASE

$P_D$ s of the clairvoyant NP receiver, the linear law and the square law non-coherent detectors versus  $\text{SNR}_{\text{eq}}$  for  $P_{FA} = 10^{-6}$  and some values of  $K$ .





# PERFORMANCE ANALYSIS: NON-COHERENT CASE

- a) The curves highlight that the larger  $K$ , the higher the detection probability.
- b) The loss of the **GLRTs** with respect to the **NP** detector becomes heavier and heavier as  $K$  increases.
- c) The performance gaps between the **square law** and the **linear detectors** are almost insignificant.
- d) Defining the integration gain as the ratio between
  - the single pulse SNR, necessary to achieve a specified detection performance for a given  $P_{FA}$  level,
  - the pre-integration SNR required such that, after integration of  $K$  pulses, the specified detection and false alarm performances are met,the gain experienced by the **GLRTs** in the non-coherent case is smaller than  $K$  which is the value corresponding to coherent detection (namely the value achieved by the **clairvoyant receiver**).



# ALBERSHEIM'S EQUATION

Albersheim's equation is an **empirical** approximation to compute the single pulse SNR,  $\chi$ , required to achieve a given  $P_D$  and  $P_{FA}$ .

## Assumptions:

- 1) Non-fluctuating target in Gaussian noise.
- 2) Linear (not square law) detector.
- 3) Non-coherent integration of  $K$  samples.
- 4) Equal target amplitudes

$$A = \ln \left( \frac{0.62}{P_{FA}} \right)$$

$$B = \ln \left( \frac{P_D}{1 - P_D} \right)$$

$$\chi_{\text{dB}} = -5 \log_{10} K + \left( 6.2 + \left( \frac{4.54}{\sqrt{K + 0.44}} \right) \right) \cdot \log_{10} (A + 0.12AB + 1.7B) \text{ dB}$$

Note that  $\chi_{\text{dB}}$  is in decibels. The error in the estimate of  $\chi_{\text{dB}}$  is less than 0.2 dB for  $10^{-7} \leq P_{FA} \leq 10^{-3}$ ,  $0.1 \leq P_D \leq 0.9$ , and  $1 \leq K \leq 8096$ .



# ALBERSHEIM'S EQUATION

Suppose  $P_D = 0.9$  and  $P_{FA} = 10^{-6}$  are required for a **non-fluctuating target** in a system using a **linear** detector. If detection is performed with a single sample, what is the required sample SNR?

Compute  $A = \ln(0.62 \times 10^6) = 13.34$  and  $B = \ln(9) = 2.197$ . With  $K=1$  the **Albersheim's** equation then gives  $\chi_{dB} = 13.11$  dB; on a linear scale this is  $\chi = 20.47$ .

If  $K = 100$  samples are **non-coherently** integrated, it should be possible to obtain the same  $P_D$  and  $P_{FA}$  with a lower single pulse SNR. To confirm this, again apply the **Albersheim's** equation but now with  $K = 100$ .

The parameters  $A$  and  $B$  are unchanged.  $\chi_{dB}$  is now -1.26 dB, a reduction of 14.4 dB. This non-coherent integration gain of 14.4 dB, a factor of 27.54 on a linear scale, is much better than the square root of  $K$  rule of thumb sometimes given for **non-coherent** integration, which would give a gain factor of only 10 for  $K = 100$  samples integrated. Rather, the gain is approximately  $K^{0.7}$  in this example.



## ALBERSHEIM'S EQUATION

If a larger error can be tolerated, Albersheim's equation can also be used for **square law** detector for non-fluctuating target and Gaussian noise.

Specifically, **square law** detector curves are within 0.2 dB of **linear** detector curves over a wide range of parameters. Thus, the same equation can be used for calculations over the range of previously given parameters with errors not exceeding 0.4 dB.

It is possible to solve the **Albersheim's** equation for either  $P_D$  or  $P_{FA}$  in terms of the other and  $\chi$  and  $K$ . For instance, the following expressions show how to estimate  $P_D$  in terms of the other factors:

$$A = \ln \left( \frac{0.62}{P_{FA}} \right), \quad Z = \frac{\chi_{1\text{dB}} + 5 \log_{10} K}{6.2 + \frac{4.54}{\sqrt{K+0.44}}}, \quad B = \frac{10^Z - A}{1.7 + 0.12A}$$

$$P_D = \frac{1}{1 + e^{-B}}$$



# RCS DECORRELATION PROPERTIES

Detection decisions are often based not on a single measurement but on a set of  $K$  measurements. For instance, the received complex voltage from a particular range bin might be measured on a series of  $K$  pulses.

When  $K$  target measurements are processed, an important question concerns how target amplitudes or powers have to be modeled:

- a single realization, selected from a given target **pdf** and repeated  $K$  times;
- $K$  different realizations selected from the same target **pdf**;
- something in the mid.

The first case is referred to as **scan-to-scan decorrelation**, while the second is referred to as **pulse-to-pulse decorrelation**.

Practically, the actual **decorrelation** behavior may lie between these two extremes, but they represent useful bounding cases for performance prediction.



# RCS DECORRELATION PROPERTIES

**RCS** decorrelation is due to changes in radar-target aspect angle or radar frequency during the time interval over which the  $K$  data samples are collected.

The change in aspect angle required to decorrelate the echo amplitude of a complex target can be estimated as:

$$\Delta\theta = \frac{c}{2L_w f} \text{ radians}$$

$L_w$  is the size of the target normal to the radar-target Line Of Sight (**LOS**), that is, the width of the target as viewed from the radar.

Successive target samples can also be decorrelated if the radar frequency is changed. The frequency step required to **decorrelate** a complex target is approximately:

$$\Delta f = \frac{c}{2L_d} \text{ Hz}$$

$L_d$  is the length of the target projected along the boresight.

Some systems deliberately change the radar frequency from pulse-to-pulse, a process called **frequency agility**, to ensure decorrelation of the target returns.



# RCS DECORRELATION PROPERTIES

As an example, consider a target size 3 m wide and 6 m long. At L-band (1 GHz), the target signature can be expected to decorrelate between 25 and 50 mrad of aspect angle rotation (about  $1.4^\circ$  to  $2.8^\circ$ ), depending on the target orientation. At X-band (10 GHz), this is reduced to only 2.5 to 5 mrad ( $0.14^\circ$  to  $0.28^\circ$ ).

The **maximum frequency step** required for decorrelation, which occurs when the target is viewed along its shortest axis, is 50 MHz. This value does not depend on the transmitted frequency.

The idea of target decorrelation is typically applied only in the context of **non-coherent** integration.

**Coherent** integration usually occurs over relatively short time intervals, and the target is generally considered to exhibit constant (but possibly random) RCS over the CPI.

Non-coherent integration often occurs over longer time periods (e. g., multiple CPIs) that are more likely to produce RCS decorrelations.



# SWERLING MODELS

To assess the performance of a radar detector, the statistical behavior of the target **RCS** is required, including both a pdf and a decorrelation model.

Together with the noise model, the **RCS** model determines the statistical characterization for the overall received samples.

**Swerling** models represent a widely accepted set of target **RCS** models.

Probability Density Function of RCS	Decorrelation	
	Scan-to-Scan	Pulse-to-Pulse
Exponential	SW1	SW 2
Chi-square, degree 4	SW 3	SW 4

P. Swerling, *Probability of detection for fluctuating targets*, IEEE Transactions on Information Theory, IT-6, 2 (Apr. 1960), 269-308.

P. Swerling, *More on detection of fluctuating targets*, IEEE Transactions on Information Theory, IT-11, 3 (July 1965), 459-460.



## FLUCTUATING TARGET

So far the developed analysis has considered only **non-fluctuating** target, also called the "**Swerling 0**", "**Swerling 5**", or "**Marcum**" case.

A more realistic model allows for target **fluctuations**, where the target RCS is drawn from either the **exponential** or **chi-square** pdf, and the RCS of  $K$  non-coherently integrated samples follows either the **pulse-to-pulse** or **scan-to-scan** decorrelation model.

The general strategy to determine **the detection probability is based on the evaluation of the conditional  $P_D$  (given the fluctuation)**. The result is then averaged over the target fluctuation.

Evidently the resulting  $P_D$  depends on the **fluctuation law** used.



# FUNDAMENTAL INTEGRAL

The following integral is necessary to address target fluctuation

$$\text{(#)} \quad \int_0^{+\infty} Q_H \left( \sqrt{2bx}, \sqrt{2T} \right) \frac{x^{\alpha-1} e^{-\frac{x}{\beta}}}{\beta^\alpha \Gamma(\alpha)} dx = \begin{cases} \sum_{n=0}^{\infty} \frac{(\alpha)_n (b\beta)^n}{(b\beta+1)^{\alpha+n} \Gamma(H+n) n!} \Gamma_{inc}(H+n, T) & \alpha > 0 \\ \sum_{n=0}^{\alpha-H} \binom{\alpha-H}{n} \frac{(b\beta)^n}{(b\beta+1)^{\alpha-H} \Gamma(H+n)} \Gamma_{inc}\left(H+n, \frac{T}{b\beta+1}\right) & \alpha \geq H \geq 1 \\ & \alpha \in \mathbb{N} \end{cases}$$

$$\Gamma_{inc}(H, x) = \Gamma(H) e^{-x} \sum_{k=0}^{H-1} \frac{x^k}{k!}$$

Incomplete Gamma Function

$$(a)_n = a(a+1)\cdots(a+n-1), \quad (a)_0 = 1$$

Pochhammer symbol

# COHERENT DETECTOR PERFORMANCE FOR GAMMA FLUCTUATING TARGET



The RCS pdf for a **Gamma fluctuating target** is

$$f_\sigma(x) = \frac{x^{\alpha-1} e^{-\frac{\alpha x}{\Omega}}}{\left(\frac{\Omega}{\alpha}\right)^\alpha \Gamma(\alpha)} u(x), \quad \alpha \geq 0 \quad \text{and} \quad \mathbb{E}[\sigma] = \Omega$$

The corresponding  $P_D$  can be obtained from (#) letting  $H = 1$ ,  $b = K$ ,  $\beta = \frac{\Omega}{\alpha\sigma^2} = \frac{\bar{\chi}}{\alpha}$

$$T = -\ln P_{FA}$$

$$P_D = \begin{cases} \sum_{n=0}^{\infty} \frac{(\alpha)_n \left(\frac{K\bar{\chi}}{\alpha}\right)^n}{\left(\frac{K\bar{\chi}}{\alpha} + 1\right)^{\alpha+n} \Gamma(1+n) n!} \Gamma_{inc}(1+n, T) & \alpha > 0 \\ \sum_{n=0}^{\alpha-1} \binom{\alpha-1}{n} \frac{\left(\frac{K\bar{\chi}}{\alpha}\right)^n}{\left(\frac{K\bar{\chi}}{\alpha} + 1\right)^{\alpha-1} \Gamma(1+n)} \Gamma_{inc}\left(1+n, \frac{T}{\frac{K\bar{\chi}}{\alpha} + 1}\right) & \alpha \geq 1, \alpha \in \mathbb{N} \end{cases}$$

where  $\bar{\chi}$  denotes the **average single pulse SNR**.

$$P_D = e^{-\frac{T}{K\bar{\chi}+1}} \quad P_D = P_{FA}^{\frac{1}{K\bar{\chi}+1}}$$

# SQUARE LAW INCOHERENT DETECTOR PERFORMANCE FOR SWERLING TARGET



$$H = K, \quad \alpha = 1, \quad \bar{\chi} = \beta = \frac{\Omega}{\sigma^2}, \quad T = \frac{\gamma}{\sigma^2} \quad (\text{Swerling 1})$$

$$P_D = \sum_{n=0}^{\infty} \frac{(K\bar{\chi})^n}{(K\bar{\chi} + 1)^{1+n} \Gamma(K+n)} \Gamma_{inc}(K+n, T)$$

$$H = K, \quad \alpha = K, \quad b = 1, \quad \bar{\chi} = \beta \quad (\text{Swerling 2})$$

$$P_D = e^{-\frac{T}{1+\bar{\chi}}} \sum_{k=0}^{N-1} \frac{1}{k!} \left( \frac{T}{1+\bar{\chi}} \right)^k$$

# SQUARE LAW INCOHERENT DETECTOR PERFORMANCE FOR SWERLING TARGET



$H = K$ ,  $\alpha = 2$ ,  $b = K$ ,  $\bar{\chi} = 2\beta$  **(Swerling 3)**

$$P_D = \sum_{n=0}^{\infty} \frac{(2)_n \left(\frac{K\bar{\chi}}{2}\right)^n}{\left(\frac{K\bar{\chi}}{2} + 1\right)^{2+n} \Gamma(K+n) n!} \Gamma_{inc}(K+n, T)$$

$H = K$ ,  $\alpha = 2K$ ,  $b = 1$ ,  $\bar{\chi} = 2\beta$  **(Swerling 4)**

$$P_D = \sum_{n=0}^{K} \binom{K}{n} \frac{\left(\frac{\bar{\chi}}{2}\right)^n}{\left(\frac{\bar{\chi}}{2} + 1\right)^K \Gamma(K+n)} \Gamma_{inc}\left(K+n, \frac{T}{\frac{\bar{\chi}}{2} + 1}\right)$$



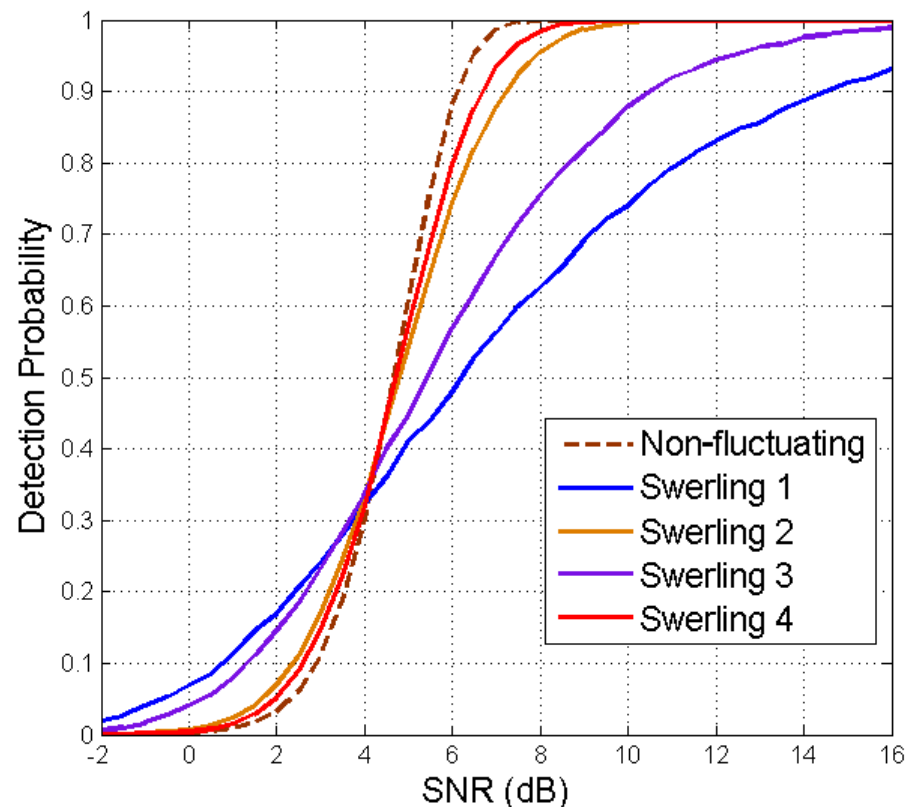
# FLUCTUATING TARGETS

The figure compares the detection performance of the four **Swerling** fluctuating targets and the **non-fluctuating** target for  $K = 10$  pulses as a function of the average single pulse SNR for a fixed  $P_{FA} = 10^{-8}$ .

For  $P_D > 0.6$ , non-fluctuating targets are easier to detect than Swerling cases; target fluctuations require a higher SNR for a given  $P_D$ .

Pulse-to-pulse fluctuations (**Swerling 2** and **4**) aid target detectability compared with scan-to-scan fluctuations.

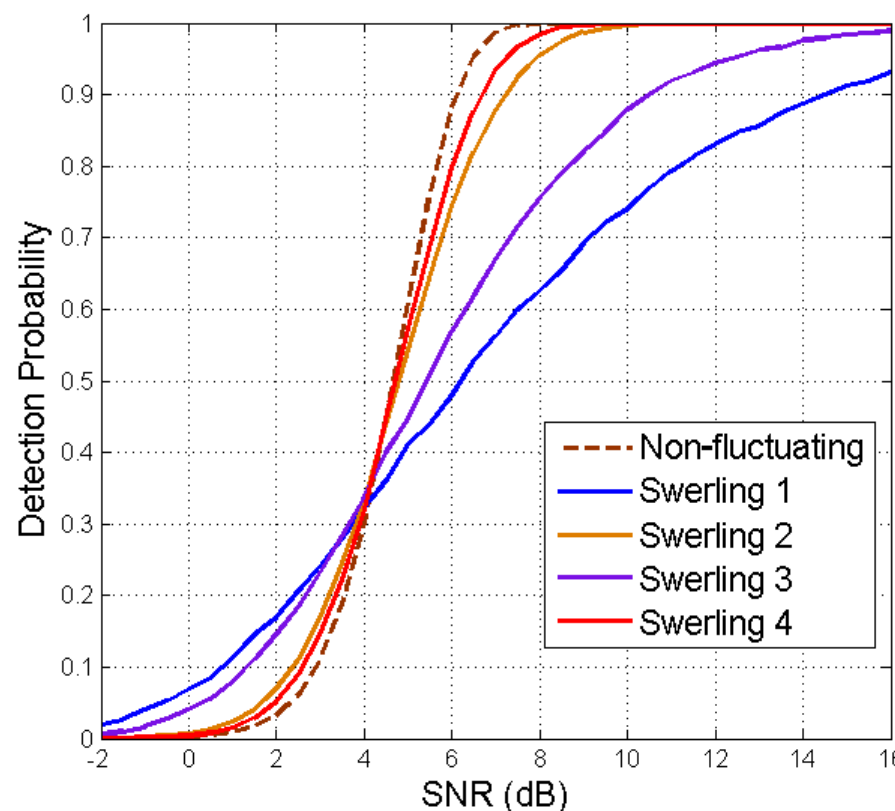
The converse of the above statements is true for **detection probabilities** less than about 0.35 (for the chosen values of the parameters).





# FREQUENCY AGILITY

For sufficiently high SNRs, if the target RCS fluctuates, it is preferable to have pulse-to-pulse fluctuations. If the radar-to-target aspect angle does not change enough during the **CPI** to decorrelate the target echoes, the radar can change the **frequency** in order to decorrelate the measurements.



# EXTENDED MODELS OF TARGET RCS STATISTICS



The results for **Swerling** models can be extended to other target amplitude pdfs. For example, a model could be defined that uses a **log-normal or Weibull pdf** for the target fluctuations with either pulse-to-pulse or scan-to-scan decorrelation to relate the  $K$  available returns.

Empirical observations have shown that “long-tailed” distributions often provide a better representation of the target data **statistics** than the traditional exponential and chi-square models, especially in high-resolution systems.

Other common pdfs (characterized by analytic tractability) include the **expanded Swerling models (non-central Gamma density), Shadowed-Rice, and correlated Gamma**.

D. J. Lewinski, *Nonstationary probabilistic target and clutter scattering models*, IEEE Transactions on Antennas and Propagation, AP-31, 3 (May 1983), 480-498.

D. A. Shnidman, *Expanded Swerling target models*, IEEE Transactions on Aerospace and Electronic Systems, 39, 3 (July 2003), 1059-1069.

A. De Maio, A. Farina, and G. Foglia, *Target fluctuation models and their application to radar performance prediction*, IEE Proceedings–Radar, Sonar and Navigation, 151, 5 (Oct. 2004), 261-269.

G. Cui, A. De Maio, and M. Piezzo *Performance Prediction of the Incoherent Radar Detector for Generalized Swerling-Chi Fluctuating Targets*, IEEE Transactions on Aerospace and Electronic Systems, 49, 1, (January 2013), 356-368.



# BINARY INTEGRATION

If the entire threshold detection process is repeated  $n$  times,  $n$  binary decisions will be available due to **multiple-dwells**.

The detection probability of a properly implemented **binary integration** detector is higher than the  $P_D$  obtained on a single detection test. Conversely, the  $P_{FA}$  is lower than the single test  $P_{FA}$ .

Thus, the **binary integration** technique can improve both detection and false alarm performance. Otherwise stated, the single dwell  $P_D$  and  $P_{FA}$  requirements can be relaxed while still meeting the overall performance specification.



## PROBLEM FORMULATION

**Problem:**  $n$  binary observations  $y_k$  are used to discriminate between the null  $H_0$  and the alternative  $H_1$  hypothesis.

The  $k$ -th observation,  $k$  in  $\{1, 2, \dots, n\}$ , is characterized by the conditional **probability mass function**  $P(y_k | H_j)$ ,  $j=0, 1$ .

The **success probabilities** under  $H_1$  and  $H_0$  are

$$P_1 \triangleq P(y_k = 1 | H_1) \quad \text{and} \quad P_0 \triangleq P(y_k = 1 | H_0)$$

**Conditionally independent observations are assumed**, i.e.

$$P(\mathbf{y}|H_j) = \prod_{k=1}^n P(y_k | H_j)$$

with  $\mathbf{y} = [y_1, \dots, y_n]^T$

$P_1$  and  $P_0$  have the meaning of **detection** and **false alarm** probabilities.



# PROBLEM FORMULATION

The problem of interest is  $H_0 : P_k = P_0; \quad H_1 : P_k = P_1;$

According to **Neyman-Pearson** criterion, the **optimum decision** statistic is derived as

$$\Lambda_{LLR} \triangleq \ln \left[ \frac{P(\mathbf{y}; P_1)}{P(\mathbf{y}; P_0)} \right] = \sum_{k=1}^n \ln \left[ \frac{P(y_k; P_1)}{P(y_k; P_0)} \right] = \sum_{k=1}^n \left\{ y_k \ln \left[ \frac{P_1}{P_0} \right] + (1 - y_k) \ln \left[ \frac{1 - P_1}{1 - P_0} \right] \right\}$$

and can be shown to be **statistically equivalent** to:  $\Lambda_{LLR} \propto \ln \left[ \frac{P_1 (1 - P_0)}{P_0 (1 - P_1)} \right] \sum_{k=1}^n y_k$

The condition  $P_1 > P_0$  automatically implies positivity of log term in last equation and the decision statistic of the **optimum test** (which is UMP) becomes

$$\sum_{k=1}^n y_k \quad \text{Binary integrator}$$



## m-OF-n DETECTION CRITERION

A number  $m$  or more detections in  $n$  trials are required before a target detection is accepted.

If  $m$  and  $n$  are properly chosen, this rule has the effect of both significantly reducing the  $P_{FA}$  and increasing the  $P_D$  compared with the single dwell case. The probability of a threshold crossing on at least  $m$ -of- $n$  tries is

$$P(m, n) = \sum_{k=m}^n \frac{n!}{k!(n-k)!} P^k (1-P)^{n-k}$$

$$H_0 : P = P_0;$$

$$H_1 : P = P_1;$$

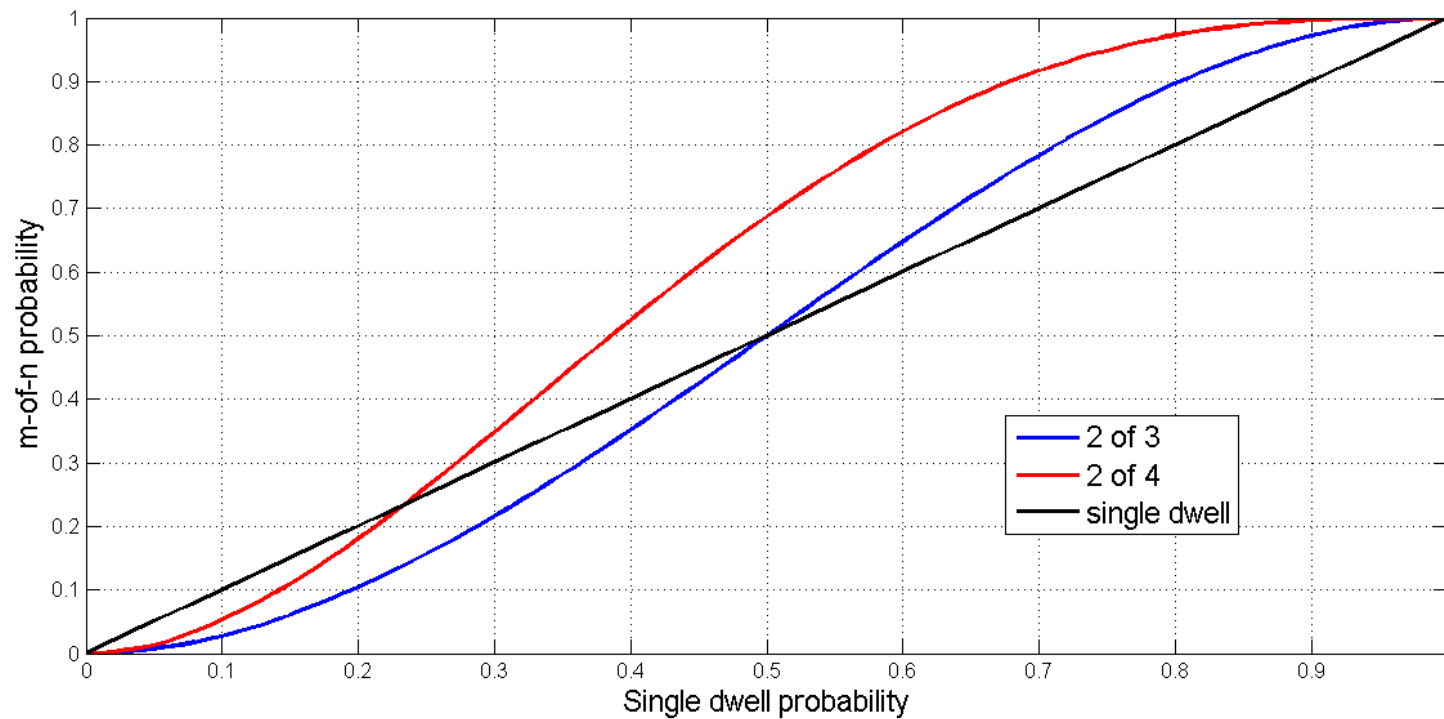
It applies to both  $P_{FA}$  and  $P_D$ . For a commonly used 2 of 3 rule ( $m = 2$ ,  $n = 3$ ) and for 2 of 4 it becomes

$$P(2, 3) = 3P^2 - 2P^3 \quad P(2, 4) = 6P^2 - 8P^3 + 3P^4$$



# m-OF-n DETECTION CRITERION

2-of-3 and 2-of-4 probability of threshold crossing versus single dwell probability.



For typical single dwell probabilities of detection (i.e., >50%), the cumulative  $P_D$  improves (increases), and for low probabilities of false alarm (i.e., <0.2) the cumulative  $P_{FA}$  also improves (decreases). The price to pay for this improvement is an extra latency before the final decision is taken.



# Part 2: *Constant False Alarm Rate Detectors*



# INTRODUCTION

Target detection involves a **thresholding** process.

If the statistics of the interference are known a-priori, a threshold may be selected to achieve a desired **probability of false alarm**.

Usually, the form of the pdf associated with the interference is known, but the parameters of the distribution are either unknown or change temporally or spatially.

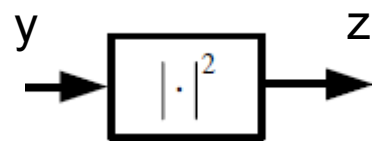
**Constant false alarm rate (CFAR) detectors** are designed **to keep a constant probability of false alarm independent of the interference pdf parameters**. Intuitively, they track changes in the interference and react adjusting the detection threshold.



## EXAMPLE: FALSE ALARM PRACTICAL IMPACT

A square law detector is commonly applied in radar systems.

Interference that is Rayleigh distributed at the output of a linear detector will be **exponentially distributed** at the output of a **square law detector**:



$$p_z(z) = \begin{cases} \frac{1}{\sigma_i^2} \exp\left(\frac{-z}{\sigma_i^2}\right) & z \geq 0 \\ 0 & z < 0 \end{cases}$$

where  $z = |y|^2$  is the output of the detector when its input is the complex interference signal  $y$ , and  $\sigma_i^2$  is the statistical average of  $z$  (**mean** interference power).



## EXAMPLE: FALSE ALARM PRACTICAL IMPACT

The probability of a false alarm is computed by integrating the pdf of  $z$  from the threshold:

$$P_{FA} = \int_T^{\infty} \frac{1}{\sigma_i^2} \exp\left(\frac{-z}{\sigma_i^2}\right) dz \quad \longrightarrow \quad P_{FA} = \exp\left(\frac{-T}{\sigma_i^2}\right)$$

**For a fixed threshold, increasing the interference power increases  $P_{FA}$ .**

**Case study:** The threshold is initially set based on a desired  $P_{FA}$  and an assumed interference power. Suppose that the actual mean interference power is increased by a factor of  $\kappa$  and that the threshold is not adjusted. The actual  $P_{FA}$  is:

$$P_{FA_{final}} = (P_{FA_{initial}})^{1/\kappa}$$

Consider an increase in the interference power by a factor of 3 dB (i.e.,  $\kappa = 2$ ):

$$P_{FA_{final}} = \sqrt{P_{FA_{initial}}}$$

For  $P_{FA_{initial}} = 10^{-6}$ , the probability of false alarm increases to  $10^{-3}$ . As expected,  $P_{FA}$  increases because the threshold is not **correctly modified** to account for the increase in the interference power.



# CFAR PROPERTY

A desirable property of a detector is the capability to keep a given **probability of false alarm** in the presence of heterogeneous or changing interference. A detector possessing this property is usually termed **CFAR**.

**Intuitive Interpretation:** CFAR detectors estimate parameters of the interference from radar measurements and **adjust the detector threshold to keep a constant  $P_{FA}$** .

When the interference power increases, an higher threshold maintains the false alarm rate at the price of a degraded detection performance.

**Please, keep in mind that there are other ways to increase the probability of detection once the threshold is adjusted.**



# CFAR THRESHOLD

The threshold of a **CFAR** detector is expressed, in general, as the product of two terms:

CFAR constant, which is a function of the desired  $P_{FA}$

$$T = \alpha \hat{g}$$

a statistic (function of measurements) associated with the interference.

This is tantamount to comparing the **normalized decision statistic**  $z/\hat{g}$  with the fixed threshold  $T$ .



## RIGOROUS DEFINITION OF CFAR

A decision rule is **CFAR** if its **pdf** under the null hypothesis  $H_0$  is functionally **independent** of the unknown **nuisance** parameters (for example the disturbance power and covariance matrix).

This implies that for a CFAR test the **detection threshold** can be set to guarantee a **preassigned**  $P_{FA}$  independently of the actual disturbance parameters.

Unfortunately, the CFAR property is not granted by a generic detection scheme.

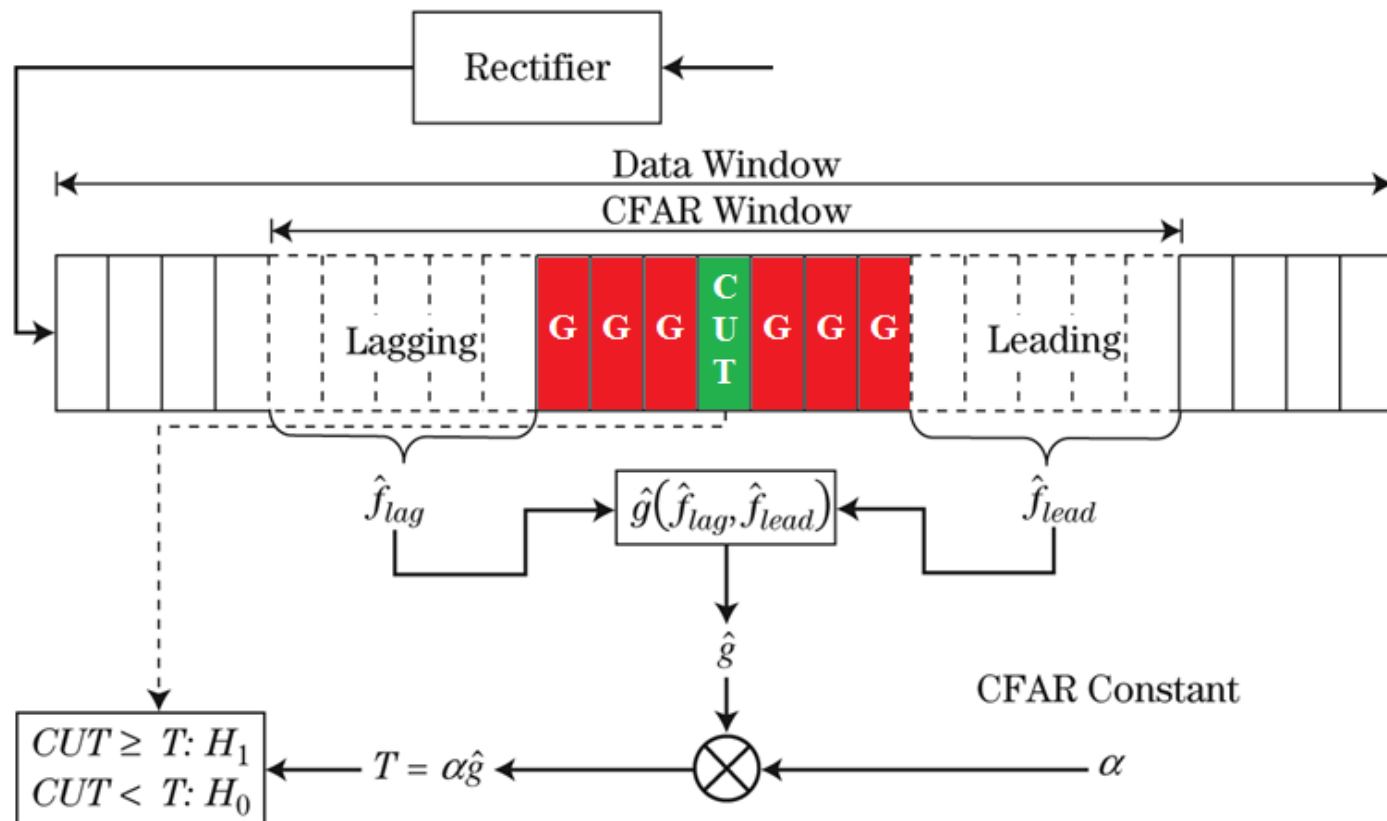
Often it is only a-posteriori verified.

There are different degrees of **CFARness** for a receiver: in the following we focus on CFAR property with respect to **interference power**.



# BASIC CFAR ARCHITECTURE

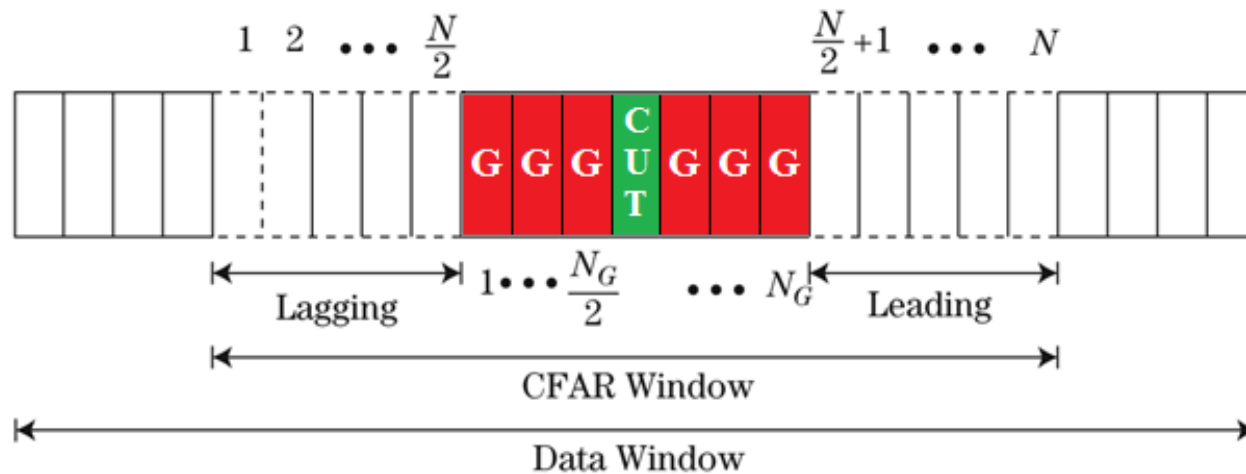
The samples at the output of the rectifier are stored in a data window. The CFAR window is composed of **leading** and **lagging** reference windows, **guard cells** (G), and a **cell under test** (CUT).





# 1-D CFAR WINDOW

An example of a one-dimensional (1-D) window is a range window consisting of **some resolutions cells**.



The **CUT** is located in the center of the **CFAR** window.

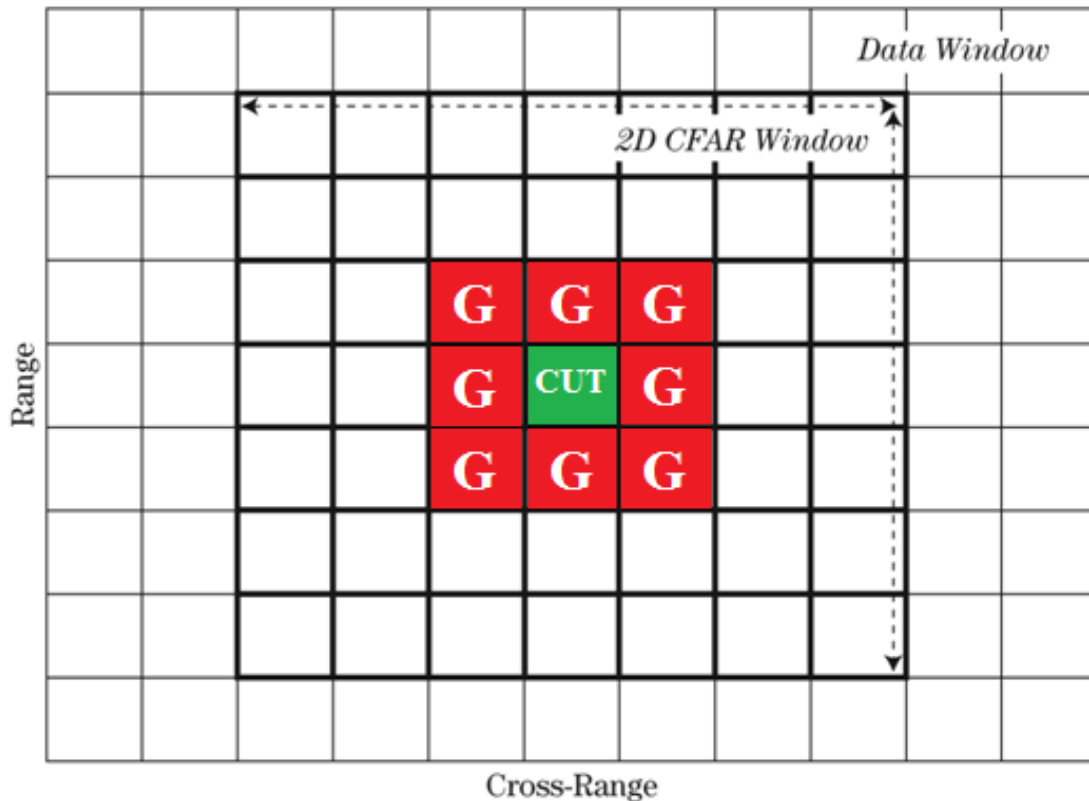
Data in the **guard cells** are not used to estimate the interference statistic (they may contain returns associated with the target in the CUT which bias the estimate).

Reference windows are located outside the guard cell region (**leading** and **lagging** windows). They are exploited to estimate the interference parameters.



## 2-D CFAR WINDOW

A 2-D data scenario and **CFAR** data window



A **2-D CFAR** is usually applied to

1. a **SAR** image to detect targets.
2. When the reference cells are from the **range-Doppler** domain



# BASIC CFAR ARCHITECTURE

The CFAR window may be implemented across

1. range,
2. Doppler,
3. angle,
4. time,
5. some combination of the aforementioned measurement domains

What is important is that the interference samples can be assumed as generally homogeneous and representative of the test sample.



# CELL AVERAGING CFAR (CA-CFAR)

**Cell Averaging CFAR computes the threshold exploiting the MLE of the average interference power obtained from the reference window.**

## Design Assumptions:

1. the interference samples in the CUT, leading, and lagging windows are i.i.d.;
2. the leading and lagging windows do not contain returns from any targets that bias the parameter estimate;
3. the interference is Rayleigh distributed in voltage.

Environments for which these conditions hold are referred to as **homogeneous**.

The **CA-CFAR** threshold and its performance are now derived (in homogeneous environment) and the further assumptions:

1. the rectifier is square law;
2. the target is modeled as either a Swerling 1 or 2 (Rayleigh amplitude).



## CA-CFAR: THRESHOLD

**Property:** the interference at the output of the square law detector is exponentially distributed.

Joint pdf of the samples  $(z_1, z_2, \dots, z_N)$  in the reference window.

$$p(z_1, z_2, \dots, z_N) = \frac{1}{(\sigma_i^2)^N} \exp\left(\frac{-\sum_{n=1}^N z_n}{\sigma_i^2}\right) \quad z_n \geq 0$$

The **MLE of the interference power** is the sample mean:

$$\widehat{\sigma}_i^2 = \frac{1}{N} \sum_{n=1}^N z_n$$



# CA-CFAR: DETECTION PROBABILITY

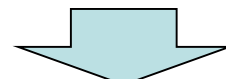
The CA-CFAR threshold is defined as

$$T_{CA} = \alpha_{CA} \widehat{\sigma}_i^2$$

Given  $(z_1, z_2, \dots, z_N)$ , the conditional  $P_D$  can be computed integrating the pdf of  $z$  (under  $H_1$ ) from  $T_{CA}$  to infinity.

pdf of  $z$  under  $H_1$

$$P_D = \int_{\alpha_{CA}}^{\infty} \frac{1}{\widehat{\sigma}_i^2(1 + SINR)} \exp\left(\frac{-z}{\widehat{\sigma}_i^2(1 + SINR)}\right) dz$$



$$P_D = \exp\left(\frac{-\alpha_{CA} \widehat{\sigma}_i^2}{\widehat{\sigma}_i^2(1 + SINR)}\right)$$



# CA-CFAR: DETECTION PROBABILITY

To compute the **unconditional probability of detection**, the conditional  $P_D$  has to be averaged over the pdf of  $\widehat{\sigma}_i^2$

$$\bar{P}_D = \int_0^{+\infty} p_{\widehat{\sigma}_i^2}(u) \exp\left(\frac{-\alpha_{CA}u}{\sigma_i^2(1 + SINR)}\right) du$$

The integral can be computed observing that it coincides with the Moment Generating Function (MGF) of  $N\widehat{\sigma}_i^2$

$$M_{N\widehat{\sigma}_i^2} = E\left[\exp\left(tN\widehat{\sigma}_i^2\right)\right], \quad t = \frac{-\alpha_{CA}}{N\sigma_i^2(1 + SINR)} \in \mathbb{R}$$

The random variable (rv) is the sum of  $N$  i.i.d. exponential rvs with parameters  $1/\sigma_i^2$

$$M_{N\widehat{\sigma}_i^2}(t) = \prod_{i=1}^N M_{z_i}(t) = M_{z_1}^N(t) = \left[1 + \frac{\alpha_{CA}}{N(1 + SINR)}\right]^{-N}$$

sum of independent rvs

identically distributed rvs

exponential distribution



# CA-CFAR: DETECTION PROBABILITY

$\bar{P}_{FA}$  is found by **setting SINR equal to zero** (interference-only condition):

$$\bar{P}_{FA} = \left[ 1 + \frac{\alpha_{CA}}{N} \right]^{-N}$$

Note that the average  $\bar{P}_{FA}$  **is independent of the interference power**. The detector thus achieves the **CFAR** property with respect to the interference power.

The **CA-CFAR** constant is found by solving for  $\alpha_{CA}$ :

$$\alpha_{CA} = N \left[ \bar{P}_{FA}^{-\frac{1}{N}} - 1 \right]$$

**Remark:** The expression for the **CFAR** constant applies only to the CA case and should not be used with other **CFAR algorithms**.



## CA-CFAR: IMPORTANT PROPERTY

CA-CFAR can be also designed resorting to the **Theory of Invariance**.

It turns out to be the

**Uniformly Most Powerful Invariant Test (UMPI)**

among all the decision rules exhibiting invariance with respect to a common scaling of the measurements and unitary transformations of training data.

**Remark:** Under some technical conditions, this property does not require the Gaussian assumption for the complex valued observations but holds true for a wide class of data distributions.



# CA-CFAR PERFORMANCE

The performance of a **CA-CFAR** is examined in terms of:

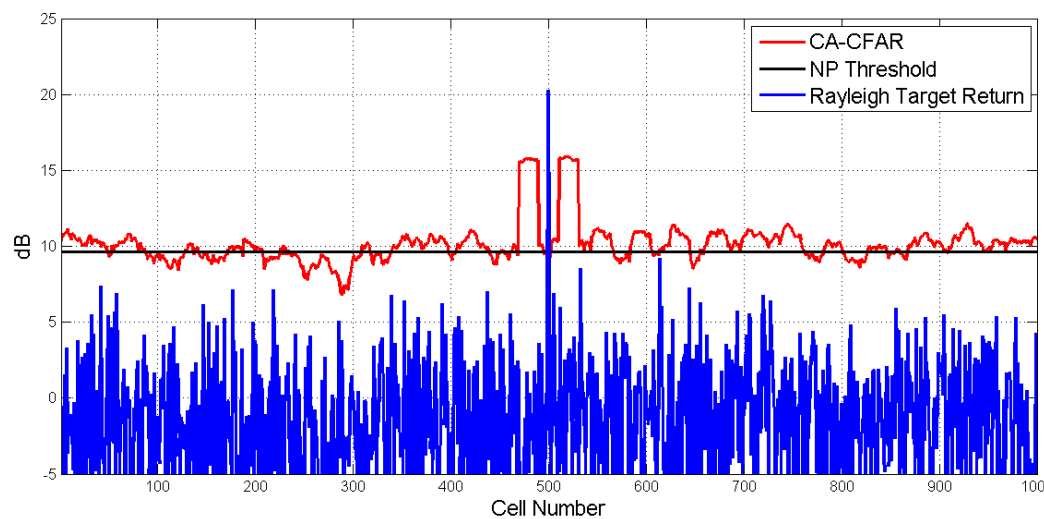
1. **CFAR loss.** The sub-optimality of the CA-CFAR implies that a  $S/NR$  greater than that associated with the NP (in the Bayesian sense with respect to uniformly distributed phase) detector is required to achieve a given  $P_D$ . In radar's jargon, the difference between the two mentioned  $S/NRs$  in dB is defined as the CFAR **loss**.
2. **Target masking.** In a heterogeneous environment, multiple targets deteriorate CFAR performance. Target returns in the reference window bias the threshold estimate and may prevent detection of the target in the CUT.
3. **Clutter boundaries.** Clutter boundaries are defined by significant and abrupt changes in the interference power. The presence of a clutter boundary can lead to an increased number of false alarms and to masking of targets located near the boundary.



# HOMOGENEOUS PERFORMANCE

Consider a single target embedded in i.i.d. interference (Rayleigh distributed with an average  $S/NR = 20$  dB). The data window consists of **1000 cells**, and a **Swerling 1 target** is in the **500th cell**. The CFAR parameters are  $N = 40$ ,  $N_G = 20$ , and  $P_{FA} = 10^{-4}$ .

The plot compares the CFAR-derived threshold (solid curve) with the NP threshold (dashed curve). The target's return exceeds both the CFAR and NP (in the Bayesian sense with respect to uniformly distributed phase) threshold.





# CFAR LOSS

The ratio between the  $SINR$  required for a CA-CFAR detector and that required for the NP detector, for a given value of  $P_D$  and  $P_{FA}$ , is defined as the CFAR loss.

## NP detector

$$P_D = \exp\left(\frac{-T}{\sigma_i^2(1 + SINR)}\right)$$

$$P_{FA} = \exp\left(\frac{-T}{\sigma_i^2}\right)$$

$$SINR_{NP} = \frac{\ln\left(\frac{P_{FA}}{P_D}\right)}{\ln(P_D)}$$

## CA-CFAR detector

$$\overline{P}_D = \left[1 + \frac{\alpha_{CA}}{N}\right]^{-N}$$

$$\overline{P}_{FA} = \left[1 + \frac{\alpha_{CA}}{N}\right]^{-N}$$

$$SINR_{CA} = \frac{\left(\frac{P_D}{P_{FA}}\right)^{1/N} - 1}{1 - (P_D)^{1/N}}$$

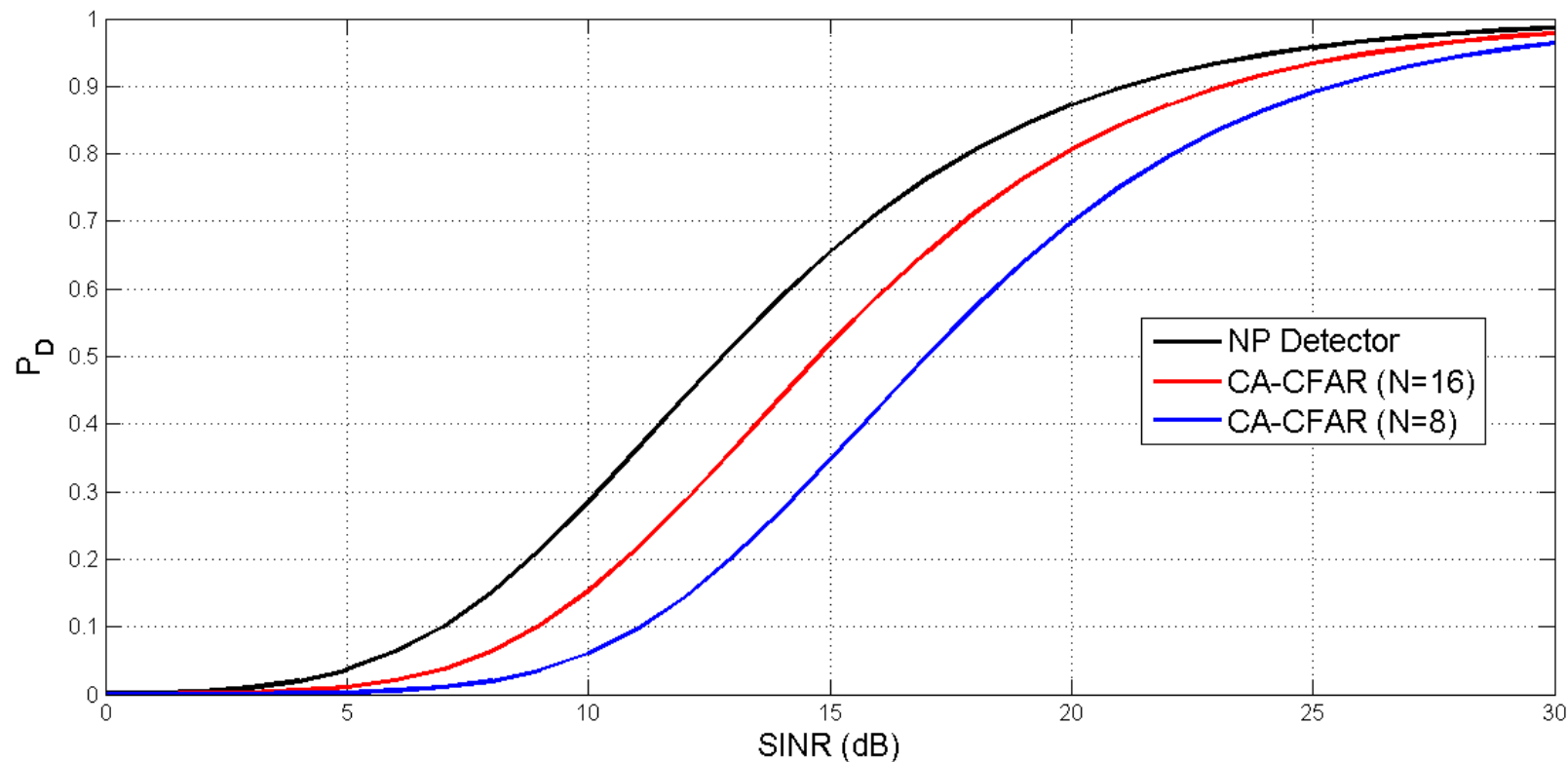
## CA-CFAR LOSS

$$L_{CA-CFAR} = \frac{SINR_{CA}}{SINR_{NP}}$$



# CFAR LOSS

The curves refer to  $P_{FA} = 10^{-6}$  and a homogeneous environment. **CFAR loss** is the difference in SINR between the two curves for a given  $P_D$ . For 90%  $P_D$ , the **CA-CFAR** loss is  $\sim 2$  dB for  $N=16$  and  $\sim 4$  dB for  $N=8$ .



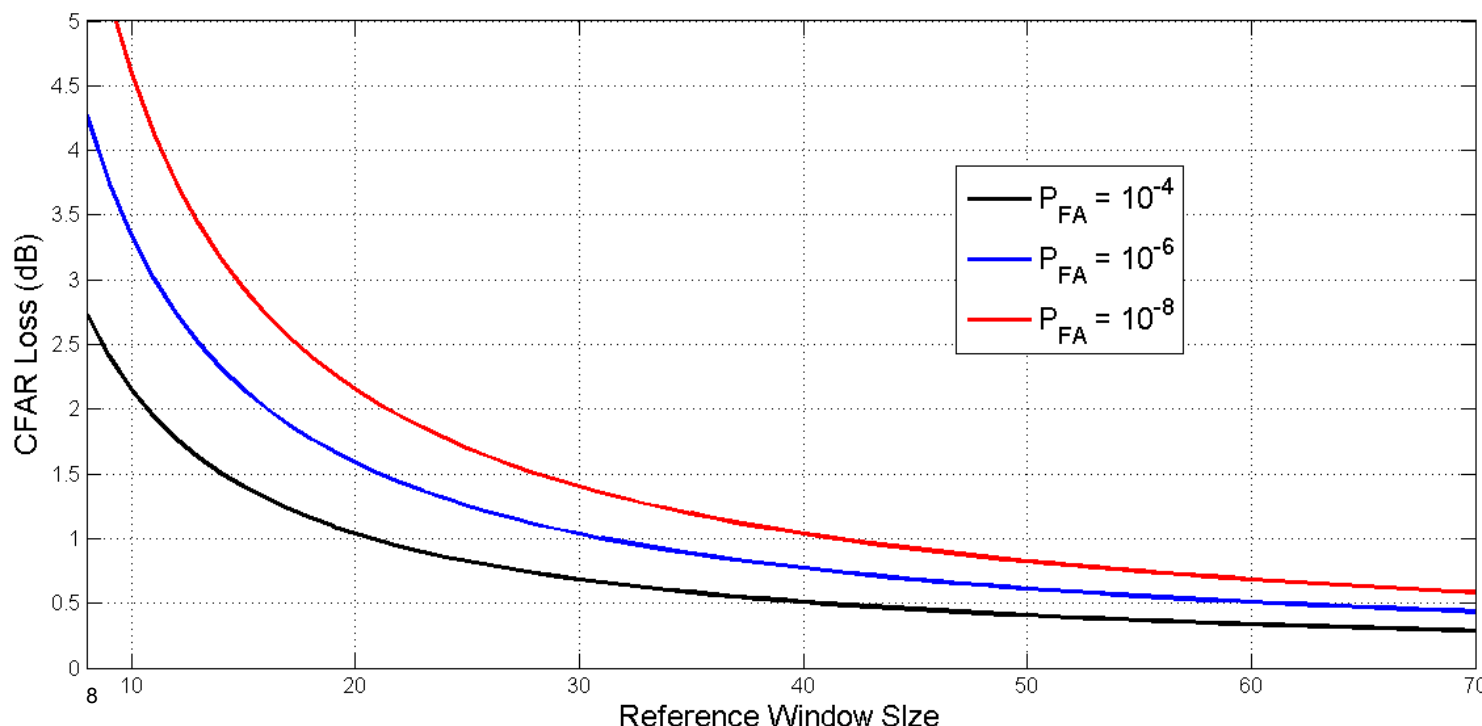


# CFAR LOSS

CFAR loss is a function of three parameters:  $P_D$ ,  $P_{FA}$ , and  $N$ .

For a given  $P_D$ , CFAR loss decreases with increasing  $P_{FA}$  and increasing  $N$ .

Dependence on  $N$  for three values of  $P_{FA}$  ( $10^{-4}$ ,  $10^{-6}$ , and  $10^{-8}$ ) and 90%  $P_D$ .





## CFAR LOSS

A large reference window could be used to minimize CFAR loss. However, when the size of the reference window increases, the probability of encountering multiple targets or a heterogeneous interference environment also increases.

For example, a large reference window increases the probability that two or more targets will belong to the CFAR window and thus increases the likelihood for mutual target masking. The number of bins comprising the reference window varies depending on the resolution of the system and the target/interference environment.

Robust CFARs are designed to operate in heterogeneous environments. The robustness of these algorithms is achieved paying in terms of CFAR loss and computational complexity.

# CA-CFAR PERFORMANCE IN HETEROGENEOUS ENVIRONMENT



**Heterogeneous** environments arise when at least one of the following is true:

1. Target returns are **present in either, or both, the leading or lagging windows** and a target is **simultaneously present in the CUT**.
2. Interference sources are **not identically distributed** within the entire reference window.

Target returns in the reference window may be due to:

1. A target located in the CUT whose physical size **occupies several resolution bins** (e.g., a 5 m length target occupying five 1 m resolution bins).
2. **Multiple targets.**

In general, these heterogeneous conditions degrade CFAR performance resulting in either a loss in  $P_D$  or increase in  $P_{FA}$ .

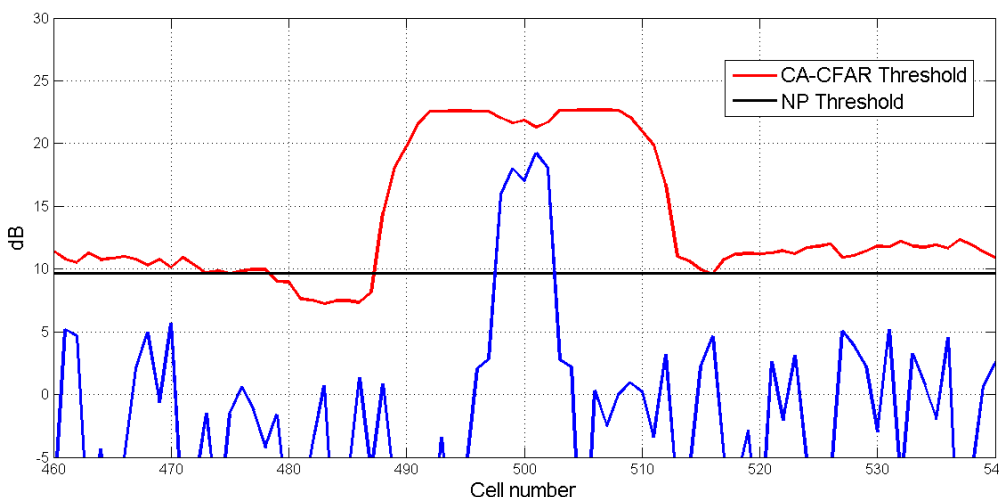


# MASKING

**Target masking** occurs when target returns located in the reference window bias the threshold above the return in the CUT.

**Self-masking** is due to an extended target (occupying more than one resolution cell). With a sample of an extended target located in the **CUT**, the remaining samples associated with the target can bias the threshold if at least one lies within the reference window.

$SINR=20$  dB for each scatterer



The extended target is composed of five Rayleigh distributed scatterers (located in different resolution cells). A **CA-CFAR** is applied with  $N = 20$  and no guard cells are considered.

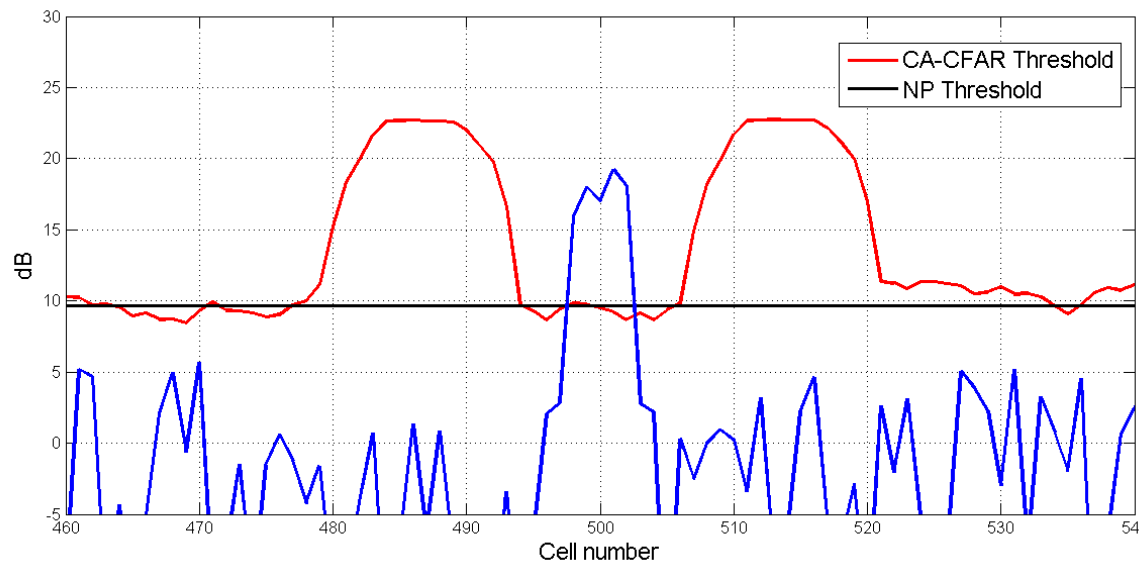
The **CFAR threshold** is biased above the target which is self-masked.



# MASKING

Guard cells can be added to both sides of the CUT to avoid self-masking.

Now the CFAR window consisting of 16 guard cells ( $N_G = 16$ ), eight on each side of the CUT, and  $N = 20$ . As is evident from the plot, the guard cells prevent self-masking.



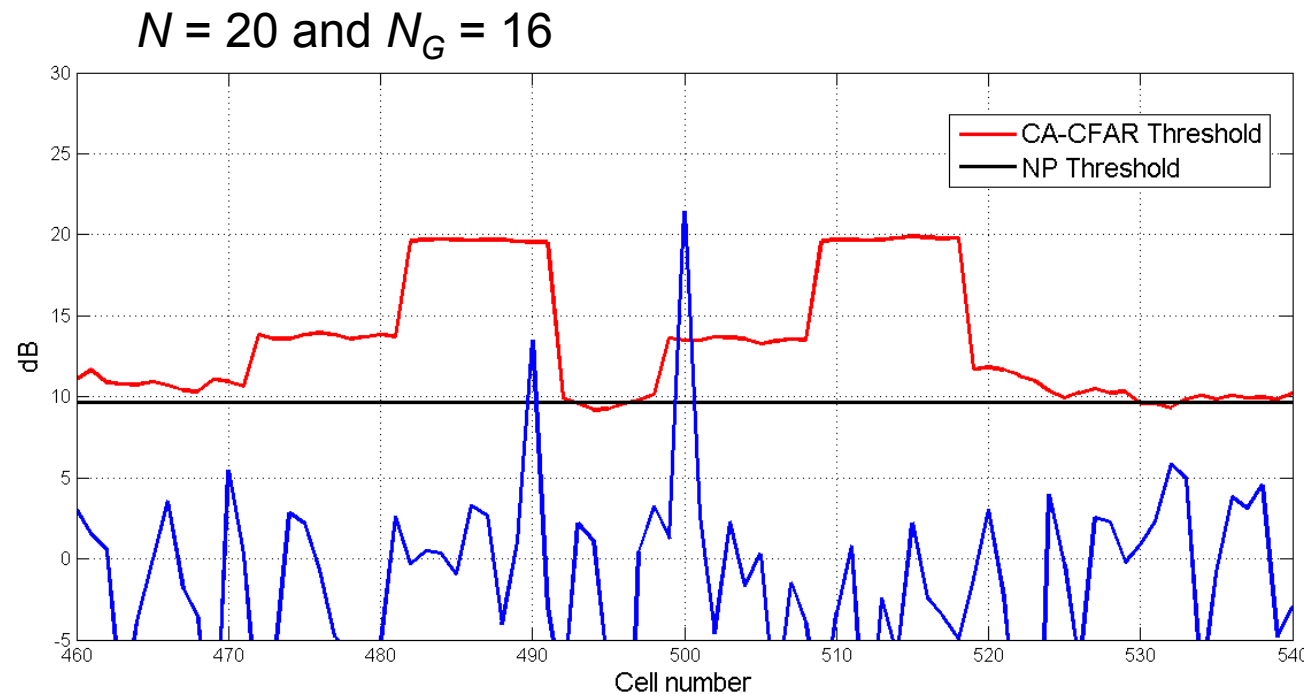
The minimum number of guard cells to place on either side of the CUT is equal to the maximum expected target's extent divided by the size of the resolution cell.



# MASKING

**Mutual target masking** happens when target returns not associated with the target in the CUT fall within the reference window and bias the threshold.

**Two Swerling 1 targets** are considered in the figure. The Swerling targets have an average  $S/NR$  equal to 20 dB. The targets are point-like and are separated by 10 resolution cells.



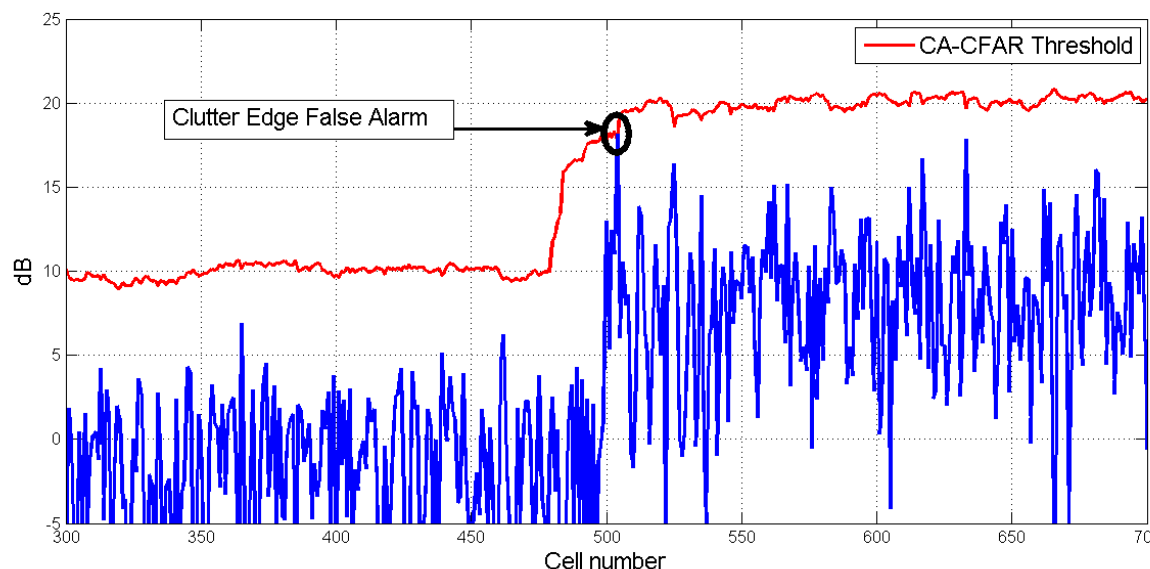


# CLUTTER BOUNDARIES (EDGES)

Abrupt changes in terrain reflectivity are termed **clutter boundaries** and represent a change in terrain type.

The presence of a clutter boundary has two main effects on CFAR performance:

1. **reduction in  $P_D$**  for targets positioned on the low reflectivity side of the clutter boundary (**clutter edge masking**);
2. **increase in the number of false alarms** near the clutter boundary. The lower reflectivity region biases the threshold down as the CFAR window passes over the clutter edge giving rise to a false alarm.





# ROBUST CFARs

**Robust** CFAR algorithms require some a-priori knowledge about the target/clutter environment (for example the maximum number of targets that could be present in the reference window).

Common robust CFAR techniques include:

- Greatest-Of CA-CFAR (**GOCA-CFAR**);
- Smallest-Of CA-CFAR (**SOCA-CFAR**);
- Trimmed Mean or Censored CFAR (**TM-CFAR**, **CS-CFAR**);
- Order Statistics CFAR (**OS-CFAR**).

GOCA-CFAR is robust with respect to clutter edge false alarms.

SOCA-CFAR, TM-CFAR or CS-CFAR, and OS-CFARs are devised to achieve robustness with respect to mutual target masking.



# GREATEST-OF CA-CFAR

**GOCA-CFAR** computes the average interference power in the lagging and leading windows separately. Then, it selects the larger between the two sample means to evaluate the adaptive threshold.

$$\hat{g}_{GO} = \max(\hat{f}_{GO,lag}, \hat{f}_{GO,lead})$$
$$\hat{f}_{GO,lag} = \sum_{i=1}^{N/2} z_i$$
$$\hat{f}_{GO,lead} = \sum_{i=N/2+1}^N z_i$$

The  $2/N$  scale factor required to compute the sample mean is included in the CFAR constant.



# GREATEST-OF CA-CFAR

In a homogenous interference environment, the average  $P_D$  of a GOCA-CFAR is:

$$P_{D_{GO}} = 2 \left\{ \left[ 1 + \frac{\alpha_{GO}}{1 + SINR} \right]^{-\frac{N}{2}} - \left[ 2 + \frac{\alpha_{GO}}{1 + SINR} \right]^{-\frac{N}{2}} \sum_{k=0}^{N/2-1} \binom{\frac{N}{2} - 1 + k}{k} \left[ 2 + \frac{\alpha_{GO}}{1 + SINR} \right]^{-k} \right\}$$

The average  $P_{FA}$  is found by setting  $SINR = 0$ :

$$P_{FA_{GO}} = 2 \left\{ [1 + \alpha_{GO}]^{-\frac{N}{2}} - [2 + \alpha_{GO}]^{-\frac{N}{2}} \sum_{k=0}^{N/2-1} \binom{\frac{N}{2} - 1 + k}{k} [2 + \alpha_{GO}]^{-k} \right\}$$

The GOCA-CFAR threshold is defined as the product between  $\hat{g}_{GO}$  and the CFAR constant embedded in the expression of the average  $P_{FA}$ .

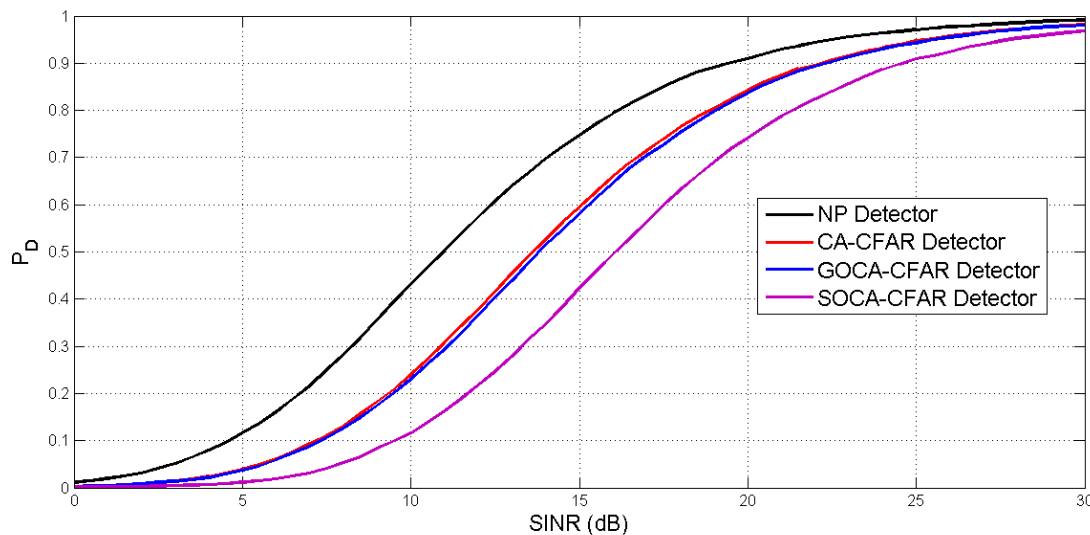
This constant computation is more difficult than the case of a CA-CFAR and involves the **iterative solution** of an equation.



# GREATEST-OF CA-CFAR

Hansen and Sawyers show that the additional CFAR loss associated with a **GOCA-CFAR** ranges between 0.1dB and 0.3 dB. This additional loss is defined relative to a CA-CFAR with the same length reference window. This holds even for small reference window sizes (e.g.,  $N = 4$ ).

ROC associated with a CA-CFAR and a GOCA-CFAR with  $N = 8$  and  $P_{FA} = 10^{-4}$ .



As expected, the ROC associated with the GOCA-CFAR appears to the right of the CA-CFAR.

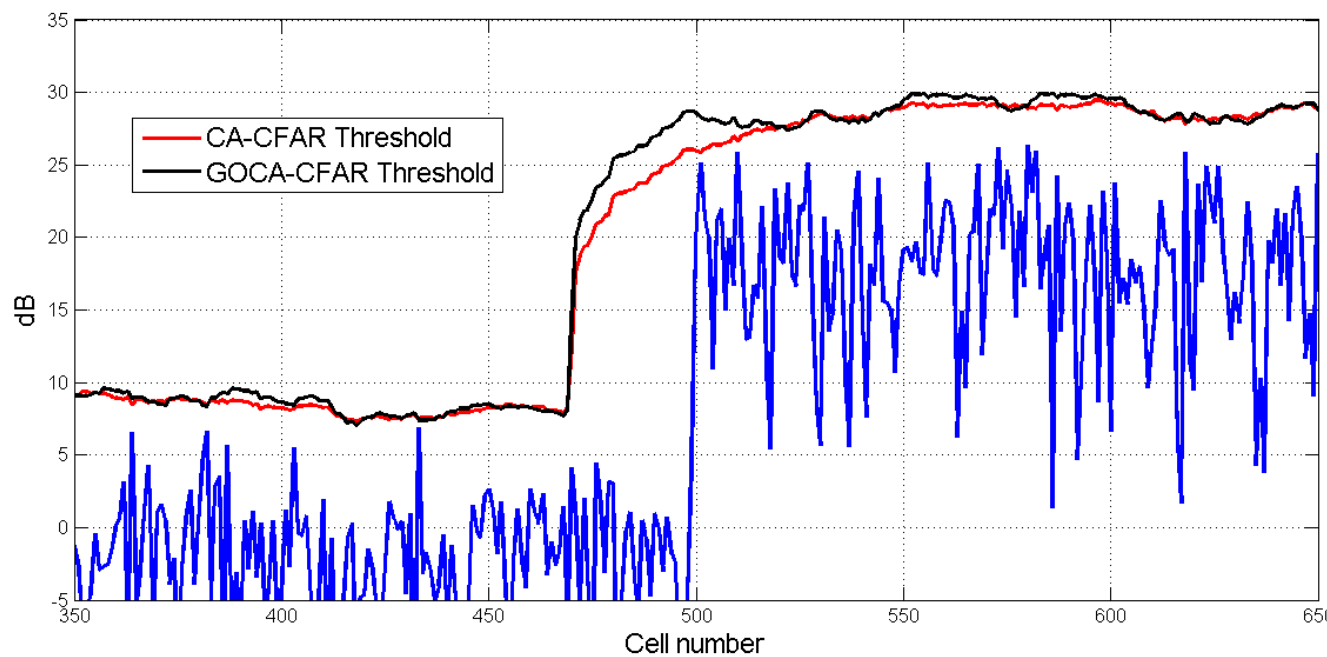
The larger CFAR loss is due to the fact that **fewer samples are used** in computing the GOCA-CFAR statistic.



# GREATEST-OF CA-CFAR

A GOCA-CFAR reduces clutter edge false alarms biasing the threshold above that of the CA-CFAR. The threshold is representative of the higher reflectivity region.

The reference window is sized for  $N = 60$ , and the desired  $P_{FA} = 10^{-3}$ .



Two clutter regions where the reflectivity between the two regions differs by 20 dB.



## SMALLEST-OF CA-CFAR

**SOCA-CFAR** computes the average interference power in the lagging and leading windows separately. Then, it selects the minimum between the two sample means to evaluate the adaptive threshold.

It suppresses interfering targets that may be located either in the leading or lagging window but not targets present simultaneously in both windows.

$$\hat{g}_{SO} = \min(\hat{f}_{SO,lag}, \hat{f}_{SO,lead})$$
$$\hat{f}_{SO,lag} = \sum_{i=1}^{N/2} z_i$$
$$\hat{f}_{SO,lead} = \sum_{i=N/2+1}^N z_i$$

The **SO** threshold is defined as:  $T_{SO} = \alpha_{SO} \hat{g}_{SO}$



# SUMMARY OF CFAR LOSSES

**CFAR loss values** recorded at the 90%  $P_D$  level for CA-CFAR, GOCA-CFAR, and SOCA-CFARs.

CFAR LOSS (dB)				
$N$	$P_{FA}$	CA-CFAR	GOCA-CFAR	SOCA-CFAR
8	$10^{-4}$	2.7	3.0	5.3
16	$10^{-4}$	1.3	1.5	2.3
24	$10^{-4}$	0.9	1.0	1.5
32	$10^{-4}$	0.6	0.8	1.0
8	$10^{-6}$	4.3	4.6	8.9
16	$10^{-6}$	2.0	2.2	3.8
24	$10^{-6}$	1.3	1.5	2.3
32	$10^{-6}$	1.0	1.1	1.7

The difference between the CA and GOCA-CFAR is **less than or equal to 0.3 dB**.



## TRIMMED MEAN OR CENSORED CA-CFAR

A **censored CFAR** orders the measured samples in the reference window and **discards the largest  $N_c$  samples** prior to computing the adaptive threshold.

Intuitively the largest  $N_c$  samples may contain returns from **interfering targets** and therefore should not be used in the estimation.

The CS-CFAR is capable of **removing  $N_c$  interfering targets** from the reference window. It is required the a-priori knowledge on the maximum number of targets that may be present in the reference window to set  $N_c$ .

For a given reference window size, augmenting  $N_c$  increases the **CFAR loss** as the number of samples used in estimating adaptive threshold decreases;

$N_c$  should be chosen accounting for the tradeoff between

- the number of potential **interfering targets**;
- the **CFAR loss** incurred.



## TRIMMED MEAN OR CENSORED CA-CFAR

A generalization of the CS-CFAR algorithm, **Trimmed Mean CFAR**, **discards the  $N_{T_L}$  largest and  $N_{T_S}$  smallest samples**.

A TM-CFAR may be configured to address different interference environments adjusting the two parameters,  $N_{T_S}$  and  $N_{T_L}$ , in correspondence of specific operating conditions.

$N_{T_L}$  is selected to remove **interfering targets**, and  $N_{T_S}$  is selected to suppress **clutter edge false alarms**.

$N_{T_L}$  is chosen based on an **a-priori estimate** of the maximum number of interfering targets in the reference window.

$N_{T_S}$  should be selected as a significant percentage of  $N$  if the goal is to minimize the effects of **clutter edge** false alarms.



# TRIMMED MEAN OR CENSORED CA-CFAR

$P_D$  and  $P_{FA}$  for both the TM-CFAR and CS-CFARs are:

$$P_{FA_{TM}} = \prod_{i=1}^{N-N_{TS}-N_{TL}} \gamma_i(\nu) \Bigg|_{\nu=\alpha_{TM}}$$

$$P_{D_{TM}} = \prod_{i=1}^{N-N_{TS}-N_{TL}} \gamma_i(\nu) \Bigg|_{\nu=\frac{\alpha_{TM}}{1+SINR}}$$

where

$$\gamma_1 = \frac{N!}{N_{TS}!(N - N_{TS} - 1)!(N - N_{TS} - N_{TL})} \sum_{k=0}^{N_L} \frac{\binom{N_{TS}}{k} (-1)^{N_{TS}-k}}{\frac{N-k}{N-N_{TS}-N_{TL}} + \nu}$$

$$\gamma_i = \frac{\frac{N-N_{TS}-i+1}{N-N_{TS}-N_{TL}-i+1}}{\frac{N-N_{TS}-i+1}{N-N_{TS}-N_{TL}-i+1} + \nu} \quad i = 2, \dots, (N - N_{TS} - N_{TL})$$

The CFAR constant contains the scale factor used to compute the sample mean.  
The CS-CFAR is a special case of the TM-CFAR with  $N_{TS} = 0$  and  $N_{TL} = N_C$ .



# ORDER STATISTICS CFAR

**OS-CFAR** orders the  $N$  samples in the CFAR reference window and selects the  $k$ -th sample as the CFAR statistic.

**OS-CFAR** is thus capable of rejecting  $N - k$  interfering targets. In addition it can suppress clutter edge false alarms provided  $k > N/2$ .

$$P_{FA_{OS}} = \prod_{i=0}^{k-1} \frac{N-i}{N-i+\alpha_{OS}}$$

$$P_{D_{OS}} = \prod_{i=0}^{k-1} \frac{N-i}{N-i+\frac{\alpha_{OS}}{1+SINR}}$$

An equivalent expression for  $P_{FA}$  is:

$$P_{FA_{OS}} = k \binom{N}{k} \frac{(k-1)!(\alpha_{OS} + N + k)!}{(\alpha_{OS} + N)!}$$

The CFAR loss associated with an OS-CFAR exhibits a relatively broad minimum as a function of  $k$ . To achieve a CFAR loss near the minimum, a reasonable value of  $k$  is  $3N/4$ . This value of  $k$  is also compatible with the suppression of  $N/4$  interfering targets.



# ORDER STATISTICS CFAR

Given  $N$ , an OS-CFAR exhibits **a CFAR loss greater** than that of a CA-CFAR.

With its **ability to suppress mutual target masking**,

1. the length of an OS-CFAR's reference window may be extended to reduce the CFAR loss;
2. the longer reference window may contain additional interfering targets, but the algorithm is capable of suppressing them;
3. similar detection performance may be achieved in a homogenous interference environment using either a **CA-CFAR** with  $N = 16$  or an **OS-CFAR** with  $N = 24$ .

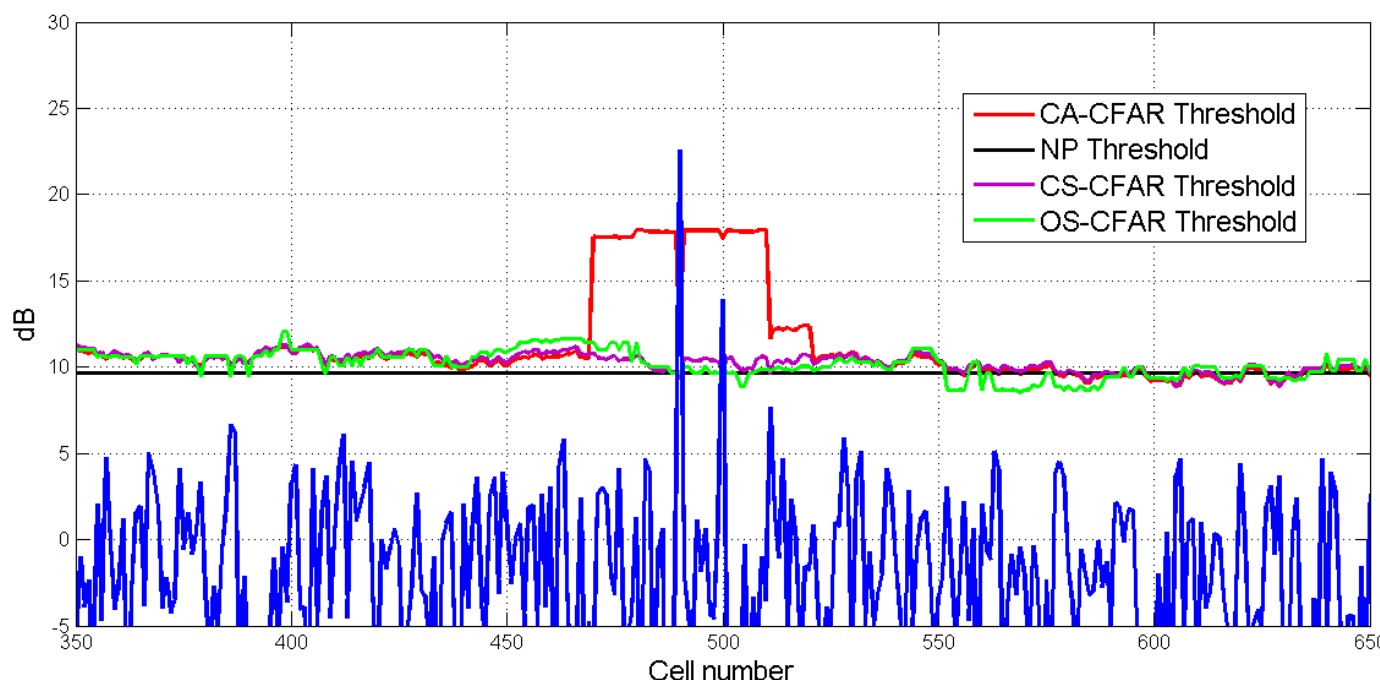
An OS-CFAR may be used to address **self-target masking**. It eliminates the need for guard cells ( $N_G = 0$ ) provided the total number of reference cells containing target returns is smaller than  $N - k$ .

**OS-CFAR** and **CA-CFAR** are special cases of the **TM-CFAR** with  $(N_{TS}, N_{TL}) = (k - 1, N - k)$  and  $(0, 0)$ , respectively.



# CS- AND OS-CFAR NUMERICAL EXAMPLE

CA-, CS-, and OS-CFAR thresholds behavior for Rayleigh distributed amplitude returns. Two Swerling 1 targets with  $S/NR=20\text{dB}$ .  $P_{FA} = 10^{-4}$ . The reference window consists of **N=40 cells**. **Nc=0 cells**. The CS-CFAR discards the largest two samples. The OS-CFAR uses the 30th sample to compute the adaptive threshold.





## COMBINING GO WITH CS OR OS

Combining greatest-of with OS- and CS-CFARs ensures robustness in the presence of multiple targets and clutter boundaries:

1. The first step is to apply either an OS- or CS-CFAR to the leading and lagging reference windows separately to address mutual target masking.
2. Next, the larger of the two statistics is then selected to suppress clutter edge false alarms.

The acronyms **GO-OS** and **GO-CS CFAR** are used to denote greatest-of order statistics and greatest-of censored CFAR.



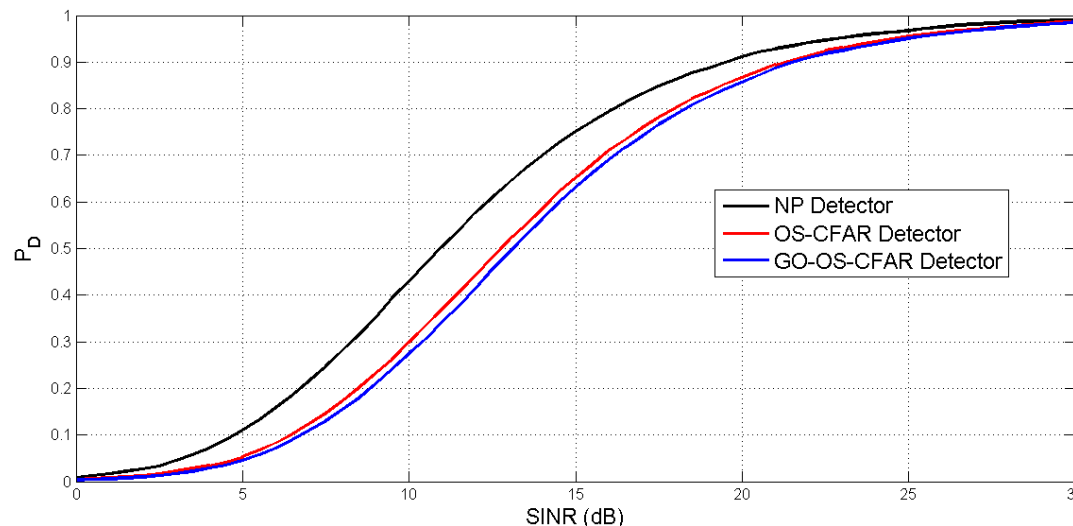
# COMBINING GO WITH CS OR OS

$P_D$  and  $P_{FA}$  of the the GO-OS CFAR:

$$P_{D_{GOOS}} = 2k^2 \left( \frac{\frac{N}{2}}{k} \right)^2 \sum_{j=0}^{\frac{N}{2}-k} \sum_{i=0}^{\frac{N}{2}-k} \binom{\frac{N}{2}-k}{j} \binom{\frac{N}{2}-k}{i} \frac{(-1)^{N-2k-j-i}}{N/2-i} \frac{\Gamma(N-j-i)\Gamma(\alpha_{GO-OS}/(1+ SINR) + 1)}{\Gamma(N-j-i + \alpha_{GO-OS}/(1+ SINR) + \frac{N}{2} + 1)}$$

$$P_{FA_{GOOS}} = 2k^2 \left( \frac{\frac{N}{2}}{k} \right)^2 \sum_{j=0}^{\frac{N}{2}-k} \sum_{i=0}^{\frac{N}{2}-k} \binom{\frac{N}{2}-k}{j} \binom{\frac{N}{2}-k}{i} \frac{(-1)^{N-2k-j-i}}{N/2-i} \frac{\Gamma(N-j-i)\Gamma(\alpha_{GO-OS} + 1)}{\Gamma(N-j-i + \alpha_{GO-OS} + N/2 + 1)}$$

The figure contains the  $P_D$  for an OS- and GO-OS CFAR. The reference window has length  $N=16$ , and  $P_{FA} = 10^{-4}$ .



The additional CFAR loss associated with combining GO and OS is only a **fraction of a dB**.

$$k_{OS}=12$$

$$k_{GOOS}=6$$



# ALGORITHM COMPARISON

The selection of a CFAR processor and its parameters is **highly dependent on the heterogeneity of the interference environment**.

1. In homogeneous environment, the CA-CFAR maximizes  $P_D$  of a scale invariant test for a given reference window size (UMPI property).
2. Heterogeneous interference significantly degrades  $P_D$  and  $P_{FA}$  performance of a CA-CFAR. In this case, **robust CFAR** techniques are required.
3. **Robust CFAR** techniques are based on a-priori knowledge of the interference environment.

ENVIRONMENT				
CFAR	Homogeneous	Interfering Targets	Clutter Boundaries	Interfering Targets and Clutter Boundaries
CA	X			
GOCA			X	
SOCA		X		
CS		X		
TM		X	X	X
OS		X	X	X
GO-OS		X	X	X
GO-CS		X	X	X



# METHODOLOGIES TO GET CFAR RECEIVERS

**CFAR property** can be obtained:

- a) properly **modifying** the decision statistic with normalization factors (or other heuristic tricks), which remove the dependence on the unknown interference parameters;
- b) **forcing** suitable symmetry properties at the design stage, which, imply CFARness.

Point b) can be accomplished by means **Theory of Invariance** in hypothesis testing which allows to focus on tests that do not distinguish among scenarios differing in their nuisance parameters.

In certain cases (not very common) the **UMPI** test exists.

Under some mild technical assumptions, the **GLRT**, the **Rao test**, and often the **Wald test** lead to invariant architectures.

A. De Maio, S. M. Kay, and A. Farina, "On the Invariance, Coincidence, and Statistical Equivalence of the GLRT, Rao Test, and Wald Test," *IEEE Transactions on Signal Processing*, Vol. 58, No. 4, pp. 1967-1979, April 2010.



## CFAR AND INVARIANCE

Applying this criterion has the effect of drastically **reducing** the problem **size** since it can be shown that all invariant test statistics can be expressed in terms of a statistic (having much fewer dimensions than the data) called the **maximal invariant**.

A **maximal invariant** statistic organizes the original data into **orbits** or **equivalence classes**.

Characterizing this statistic greatly facilitates and sometimes completes the search for a good test statistic.

The distribution of the **maximal invariant** is parameterized by another low-dimensional function on the parameter space (called the **induced maximal invariant**). By doing so, most of the nuisance parameters are removed from the problem.



## REFERENCES

The common denominator of this talk is the **detection theory** (or **hypothesis testing**) which is a branch of the statistical signal processing. A domain of application for detection theory is in the context of radar, sonar systems and, sensing systems.

The book by **Lehman** [a] represents a relevant contribution to the hypothesis testing and treats the mathematical foundations of hypothesis testing and parameter estimation.

The works by **Kay** [b], [c] strike a balance between highly theoretical expositions and the more practical treatments, focusing extensively on real-world signal processing applications.

These works are complementary and oriented to practicing electrical engineers, users, managers, PhD students, as well as researchers, providing an invaluable introduction to parameter estimation and detection theory.

- a) E. L. Lehmann, *Testing Statistical Hypotheses*, Springer-Verlag, 2nd edition, 1986.
- b) S. M. Kay, *Fundamentals of Statistical Signal Processing, Detection Theory*, Englewood Cliffs, NJ: Prentice-Hall, 1998, vol. II.
- c) S. M. Kay, *Fundamentals of Statistical Signal Processing, Estimation Theory*, Upper Saddle River, NJ: Prentice-Hall, 1993, vol. I.



## REFERENCES

The book by **Van Trees** [d] applies hypothesis testing and parameter estimation to detection, estimation, and modulation of continuous-time waveforms.

Influential and scholarly engineering texts are the book by **Scharf** [e] and **Helstrom** [f]. The former covers three distinct topical lines: detection theory, estimation theory, and time series analysis. The latter focuses on concepts of signal detection, maintaining a good balance between mathematical rigor and practical applications.

Reference [g] contains three very well written chapters, related to this talk, focused on **search radars**, **radar detection**, and **CFAR** techniques (Chapters 3 -15-16). Finally, textbooks [h]–[j] deal with several aspects of modern radar detection systems and are oriented to the radar engineers focused on the application.

- d) H. L. Van Trees, *Detection, Estimation, and Modulation Theory, Part I*, John Wiley & Sons, 2002 (1968).
- e) L. L. Scharf, *Statistical Signal Processing: Detection, Estimation, and Time Series Analysis*, Addison-Wesley, 1991.
- f) C. W. Helstrom, *Elements of Signal Detection and Estimation*, Prentice Hall PTR, 1994.
- g) M. A. Richards, J. A. Scheer, and W. A. Holm, *Principles of Modern Radar: Basic Principles*, Scitech Publishing, Raleigh NC, 2010.
- h) D. K. Barton, *Radar System Analysis and Modeling*, Artech House, Norwood, MA, 2005.
- i) M. I. Skolnik, *Introduction to Radar Systems*, 3d ed., McGraw-Hill, New York, 2001.
- j) A. De Maio and M. S. Greco, *Modern Radar Detection Theory*, Scitech Publishing, 2016.



# ACKNOWLEDGEMENT

The authors thank for the helpful discussions and suggestions:

- **Dr. V. Carotenuto** (University of Napoli “Federico II”, Italy)
- **Prof. E. Conte** (University of Napoli “Federico II”, Italy)
- **Prof. G. Cui** (University of Electronic Science and Technology, China)
- **Dr. A. Farina** (Consultant, previously with Selex-ES Italy)
- **Prof. D. Orlando** (Università “Niccolò Cusano”, Italy)
- **Dr. Luca Pallotta** (University of Napoli “Federico II”, Italy)

The speakers also thank the **authors** of the many references developed along the years who have made possible the preparation of this tutorial.



*Thank you for  
the kind attention*

*End Session*



## APPENDIX: SUFFICIENT STATISTICS

Consider a random variable  $X \sim \mathcal{P}_\theta$  where  $\mathcal{P}_\theta$  refers to the class of pdfs indexed by the parameter  $\theta$

**Definition 1 (Sufficiency).** A statistic  $T(X)$  is sufficient for  $\theta$  iff the conditional distribution of  $X$  given  $T = t$  does not depend on  $\theta$ .

**Theorem 1 (Factorization Criterion).**  $T$  is sufficient for the parameter  $\theta$  of the family of distributions generating  $X$  iff the densities of  $X$  satisfy

$$p_\theta(x) = g_\theta[T(x)]h(x).$$

**Definition 2 (Minimal Sufficiency).** A sufficient statistic  $T$  is minimal sufficient if for any sufficient statistic  $U$  there exists a function  $h$  such that  $T = h(U)$ .



## APPENDIX: EXPONENTIAL FAMILIES

**Definition 3** (*s*-parameter exponential families). *A class of distributions  $\mathcal{P}_\theta = \{P_\theta\}$  is an *s*-parameter exponential family if the densities of the members of the class have the form*

$$p_\theta(x) = \exp \left[ \sum_{i=1}^s \theta_i T_i(x) - A(\theta) \right] h(x),$$

*where  $\theta = (\theta_1, \dots, \theta_s)' \in E_s$ . If the  $\theta_i$  are linearly independent and the  $T_i$  are also linearly independent then the family is full-rank exponential.*

**Theorem 2.** *If  $p_\theta(x)$  is the density of a full-rank *s*-parameter exponential family, then  $T(x) = (T_1(x), \dots, T_s(x))'$  is minimal sufficient.*